STRONG FLOWS OF VISCOELASTIC WORMLIKE MICELLE SOLUTIONS

Jonathan P. Rothstein

Department of Mechanical and Industrial Engineering,
University of Massachusetts, Amherst, MA 01003 USA

E-mail: rothstein@ecs.umass.edu

ABSTRACT

The unique rheological properties of viscoelastic wormlike micelle solutions have led to their broad use as rheological modifiers in consumer products such as paints, detergents, pharmaceuticals, lubricants and emulsifiers. In addition, micelle solutions have also become increasingly important in a wide range of industrial and commercial applications including agrochemical spraying, inkjet printing, turbulent drag reduction and enhanced oil recovery. Until recently, our knowledge of the rheology and flow behavior of these fluids was limited to linear viscoelasticity measurements where wormlike micelle solutions have been shown to behave as ideal Maxwell fluids, and steady shear rheology measurements where wormlike micelles often demonstrate shear banding. In this review, we survey recent experimental and theoretical developments for nonlinear rheology of viscoelastic wormlike micelle solutions and the response of these complex fluids to strong flows. Specific emphasis will be placed on extensional rheology measurements and complex flows having strong extensional components. In many of these flows, viscoelastic wormlike micelle solutions behave in a manner very similar to polymer solutions. Wormlike micelle solutions demonstrate strain hardening of their extensional viscosity which can result in an increased resistance to complex flows such as the flow past a sphere or the flow through porous media. Additionally, the large extensional viscosity of these fluids has led to significant drag reduction in turbulent flows. However, wormlike micelles are self-assembled and as such are quite different than polymer solutions. Under large elastic stresses, wormlike micelles can break apart. This failure and the resulting morphological changes have been linked to a number of newly discovered elastic instabilities not present in polymer solutions. As this review will show, strong flows of wormlike micelle solutions hold a wealth of interesting flow phenomena much of which is yet to be explored.

KEYWORDS: Surfactant solutions; Viscoelastic wormlike micelle solutions; Extensional rheology; Shear rheology; Elastic instabilities.

1. INTRODUCTION

A number of recent review articles have been written on the rheology and applications of wormlike micelle solutions [1-5]. In this review, we intend to focus less on the linear viscoelasticity of these fluids and more on the strong flows that are found in a number of industries and applications for which wormlike micelle solutions are commonly used.

Surfactants are amphiphilic molecules which have both a bulky hydrophilic head, which is often charged, and a relatively short and slender hydrophobic tail typically consisting of an 8-20 carbon atom chain. Above their critical micelle concentration (CMC), surfactant molecules in water will spontaneously self-assemble into large aggregates known as micelles to minimize the exposure of their tails to water [6-8]. In oil, reverse micelles are formed where instead the head-groups are shielded from the oil [9,10]. As seen in Figure 1, these large aggregates can form into a number of different complex shapes including spherical and wormlike micelles, vesicles and lipid bilayers [11]. The morphology of the aggregates depends on the size of the surfactant head group, the length and number of tails, the charge on the surfactant, the salinity of the solution, temperature, and the flow conditions [6,11]. Surfactants with a large head group and/or a single short tail tend to form spherical micelles while surfactants with small head groups and/or a single long tail tend to form wormlike micelles. Surfactants with two or more tails tend to form bilayers. The basis for these relatively simple distinctions are made quite clearly by Isrealachvili [12] using a packing argument based on the relative effective size of the surfactant head and tail groups.

The phase diagram of surfactant solutions that form wormlike micelle solutions can be quite complex [11,13]. As the concentration of surfactant in solution is increased, a transition is observed from dilute individual micelles, to semi-dilute entangled micelles, to nematic, hexagonal, cubic or other ordered phases at the highest surfactant concentrations. Within the semi-dilute regime, increasing salt concentration can drive the wormlike micelles from linear, to branched and finally to an interconnected saturated network. For a linear wormlike micelle, the shape and area

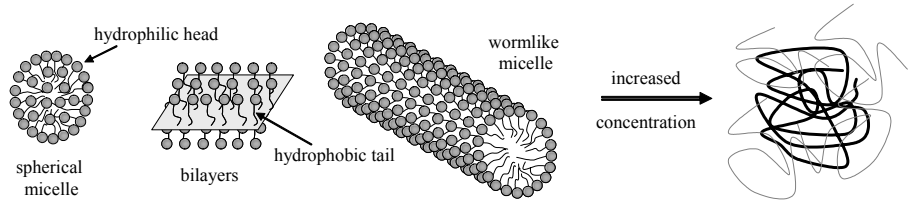

Figure 1: Schematic diagram of surfactant solutions showing various morphologies including spherical micelles, bilayers, wormlike micelles and entangled wormlike micelles which can impart viscoelasticity to the fluid.

per unit surfactant molecule is optimized at all positions along the backbone except at the endcaps [6]. When a linear micelle breaks, it must pay an energy penalty by forming two new end caps. In this regime, the electrostatic repulsion of the head groups is strong enough that the increased curvature of an endcap, which spreads the head groups apart, is favored over the concave curvature of a branch point which drives the charged head groups of the surfactants closer together. However, as the salt concentration is increased and the head group charges are sufficiently screened, the wormlike micelles can form three-point or four-point junctions. Evidence of the existence of these branched micelles can be seen in cryo-TEM images [14-18].

This review will focus on surfactants that tend to form either linear or branched wormlike micelles because at large surfactant concentrations these wormlike micelles can grow very long, become entangled, and make the solution viscoelastic. As suggested by their pseudonym 'living polymers,' wormlike micelles display many of the same viscoelastic properties of polymers. However, although both wormlike micelle solutions and polymer solutions can be viscoelastic, wormlike micelles are physically quite different from polymers. Whereas the backbone of a polymer is covalently bonded and rigid, wormlike micelles are held together by relatively-weak physical attractions and as a result are continuously breaking and reforming with time. In an entangled network, both individual polymer chains and wormlike micelles can relieve stress through reptation driven by Brownian motion [7]. However, unlike polymeric fluids, wormlike micelle solutions have access to a number of stress relief mechanisms in addition to reptation. Wormlike micelles can relieve stress and eliminate entanglement points by either breaking and reforming in a lower stress state [8] or alternatively by creating a temporary branch point which allows two entangled micelles to pull right through each other thereby eliminating the entanglement point and relieving stress in what has become known as a 'ghost-like' crossing [19].

Viscoelastic wormlike micelle solutions are currently being used extensively as rheological modifiers in consumer products such as paints, detergents, pharmaceuticals, lubricants and emulsifiers where careful control of the fluid properties are required. In addition, micelle solutions have also become important in a wide range of applications including agrochemical spraying, inkjet printing, turbulent drag reduction and enhanced oil recovery where they are often used as a polymer-free fracture fluid for stimulating oil production [1,2,20]. A fundamental understanding of the behavior of these complex fluids in different flow regimes is therefore extremely important to a host of industries. Techniques for the analysis and control of the flow of complex fluids require accurate determination of material properties as well as the ability to understand and predict changes that occur within the materials as they are subjected to the flow conditions encountered in industrial and commercial applications. Shear and extensional rheometers provide an excellent framework for investigating the behavior of these complex fluids because the flow kinematics tends to be simple. Additionally, these rheological measurements can shed light on the dynamics of wormlike micelle solutions in complex flows and phenomena such as elastic flow instabilities, which commonly occur in many of the industrial and commercial applications mentioned above. A number of studies of the nonlinear

rheology and the behavior of these complex fluids in strong flows have recently been published. It is the aim of this review to summarize the results of those studies.

The outline of this review is as follows. In Section 2, we discuss the shear rheology of wormlike micelle solutions. In Section 3, we discuss extensional rheology measurements. In Section 4, we discuss complex flows of wormlike micelle solutions. Finally, in Section 5 we conclude and present our outlook for future research in this area.

2. SHEAR RHEOLOGY OF WORMLIKE MICELLE SOLUTIONS

2.1. Linear Viscoelasticity

One of the observations that sparked the initial rheological interest in wormlike micelle solutions was that their linear viscoelastic response can often be quite accurately modeled by a Maxwell model having just one or two relaxation times [8,21]. The discrete multi-mode Maxwell spectrum is given by Equations 1 and 2,

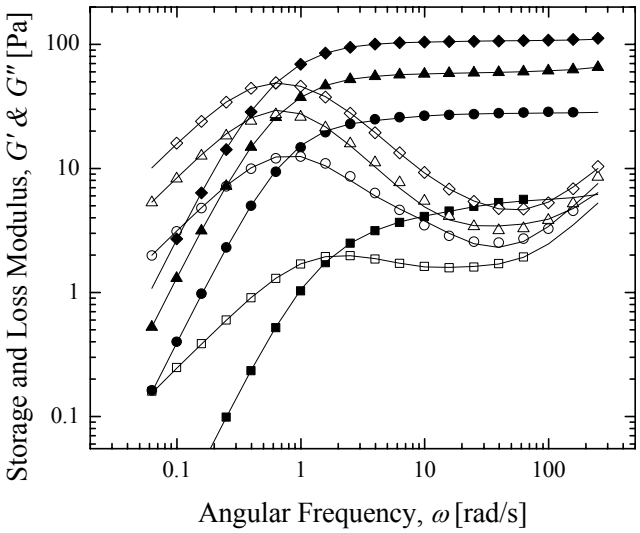

Figure 2: Small amplitude oscillatory rheology of CPyCl/NaSal solutions in 100mM NaCl at T = 20°C. The data include: storage modulus, G' (filled symbols), and loss modulus, G" (open symbols), for '■' 50/25mM, '●' 100/50mM, '▲' 150/75mM, and '♦' 200/100mM with two-mode Maxwell model fits to each of the data sets (−). (Adapted from Figure 2 of Ref. [23])

$$G' = \sum_{i=1}^{n} \frac{\eta_i \lambda_i \omega^2}{1+(\lambda_i \omega)^2} = \sum_{i=1}^{n} \frac{G_i (\lambda_i \omega)^2}{1+(\lambda_i \omega)^2} \quad (1)$$

$$G'' = \sum_{i=1}^{n} \frac{\eta_i \omega}{1+(\lambda_i \omega)^2} = \sum_{i=1}^{n} \frac{G_i \lambda_i \omega}{1+(\lambda_i \omega)^2} \quad (2)$$

where G' and G'' are the loss and storage moduli respectively, λ_i are the discrete relaxation times, η_i are the discrete viscosities and ω is the angular velocity [22]. Dividing the viscosity by the relaxation time we get the modulus of each mode of the fluid, $G_i = \eta_i / \lambda_i$. In Figure 2, the linear viscoelastic response of a number of different wormlike micelle solutions are presented [23,24]. The solutions consist of a number of different concentrations of the cationic surfactant cetylpyridinium chloride (CPyCl) and sodium salicylate (NaSal) in an aqueous solution of 100mM sodium chloride (NaCl). In Figure 2, the molar ratio of surfactant to salt is fixed at 2:1. Superimposed over the data in Figure 2 is a two-mode Maxwell model fit which is in excellent agreement with the data. It should be noted that the relaxation times of the two modes are far enough apart for these fluids that a single-mode Maxwell model would adequately fit the data at low angular frequencies. These data are but one example demonstrating the ideal flow behavior of these fluids in the linear flow regime [8,13,21,25-32]. From the elastic modulus, a theoretical mesh size or correlation length of the entangled micelles can be calculated from elastic network theory, $\xi = (k_B T / G_0)^{1/3}$, where k_B is the Boltzmann constant and T is the temperature [33,34]. The mesh size is a good measure of the proximity of entanglements and density of the wormlike micelle mesh.

Over the last two decades, Cates and coworkers have developed constitutive models which describe with excellent agreement the linear viscoelastic response of wormlike micelles [4,28,34,35]. Their model assumes two distinct relaxation mechanisms for the wormlike micelle chain; a break-up of the wormlike micelle that can occur with equal likelihood at any point along the chain and the reptation of the micelle through its confinement tube. The reptation and break-up relaxation mechanisms have characteristic time scales of λ_{rep} and λ_{br}, respectively. In the fast-breaking limit, where the break-up time is much shorter than the reptation time, $\lambda_{br} \ll \lambda_{rep}$, Cates' model [36] predicts that the linear viscoelastic response of these wormlike micelle solutions can be described by Maxwell fluids with a single relaxation time that is the geometric mean of the reptation and break-up time, $\lambda = (\lambda_{rep} \lambda_{br})^{1/2}$. Furthermore, in this regime Cates and Candau [35] developed a scaling for the relaxation time, elastic modulus and zero shear rate viscosity with volume fraction, ϕ, of surfactant zzz

$$\lambda = (\lambda_{rep} \lambda_{br})^{1/2} \sim \phi^{1.5}, \quad (3)$$

$$G_0 \sim \phi^2, \quad (4)$$

$$\eta_0 = G_0 \lambda \sim \phi^{3.5}. \quad (5)$$

The results of this scaling analysis have been shown to match the experimental data for a number of systems with very good agreement [37]. However, for systems with strongly binding counterions like Sal^- and for wormlike micelle solutions that exhibit some degree of branching, the scaling of the viscosity and relaxation time with surfactant concentration often breaks down even as the modulus continues to follow the quadratic scaling with volume fraction [26,27,32,38]. The effect of salt concentration on the rheology of the wormlike micelle solutions can be quite complex; the viscosity and relaxation time are often non-monotonic functions of salt concentration [8,26,27,39].

As seen in Figure 2, the linear viscoelastic data are not always easily fit by a single relaxation time. Granek and Cates [34] showed that that the high frequency deviations can be accounted for by Rouse-like relaxation modes and primitive path fluctuations along the micelle chain. In Figure 3, the deviation from a single-mode Maxwell fluid is emphasized by presenting the data as a Cole-Cole plot with the normalized storage modulus, G''/G_0, plotted against the normalized loss modulus, G'/G_0. The agreement between the linear viscoelastic data and the predictions of the single-mode Maxwell model improves with increasing surfactant concentration. Kern *et al*. [40] showed the break-up time of the wormlike micelles, λ_{br}, roughly corresponds to the angular frequency at which the data deviates from the predictions of the single-mode Maxwell model. Values of the break-up time have been found for a number of different wormlike micelle solutions and typically vary between several tens of milliseconds to several hundred milliseconds [41]. Additionally, Kern *et al.* [40] showed that the number of entanglements per wormlike micelle can be

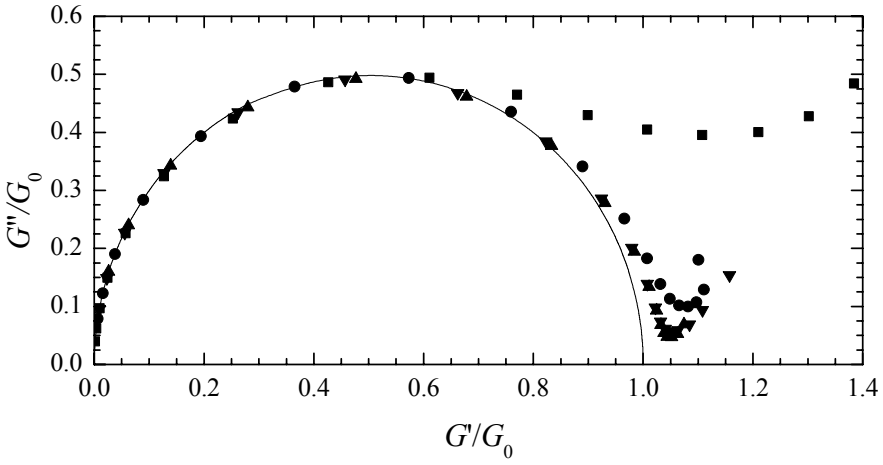

Figure 3: Cole-Cole plot of the data presented in Figure 2. The semicircle superimposed over the data represents the predictions of a single-mode Maxwell model.

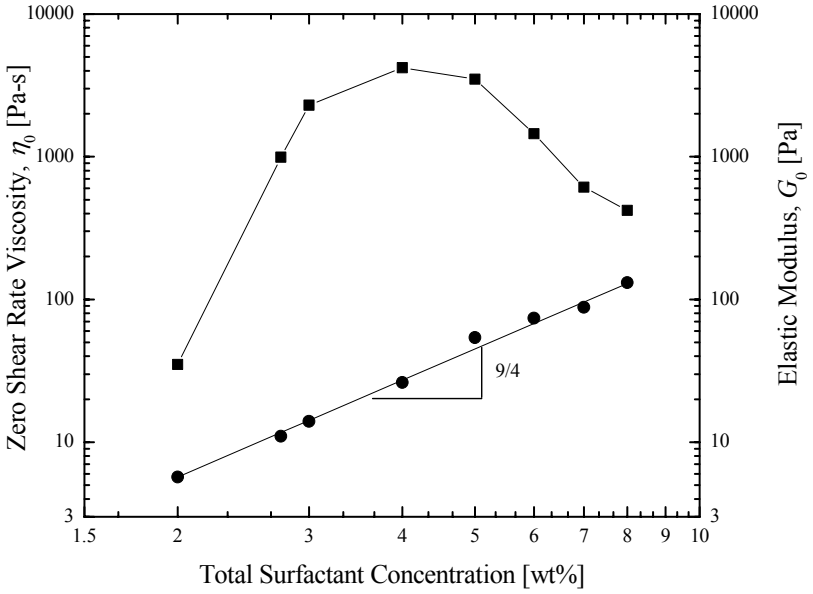

Figure 4: Steady shear rheology measurements of 70/30 NaOA/C_8TAB mixtures as a function of total surfactant concentrations at T= 23°C. The data include: ! the zero shear rate viscosity, η_0, and , the elastic modulus, G_0. (Adapted from Figure 4 of Ref. [45])

approximated by the inverse of the high-frequency minimum in the normalized storage modulus.

A number of branched wormlike micelle systems have been developed recently and their shear rheology has been well characterized [19,31,32,42-33]. In this review, we have chosen to focus on the mixed anionic and cationic surfactants pioneered by Raghavan and Kaler [32,43] because the systems they developed have viscosities and relaxation times suitable for extensional rheology measurements using either a filament stretching rheometer (FiSER) or a capillary break-up rheometer (CaBER) which we will describe in the following sections [45]. Raghavan *et al*. [32] produced a series of wormlike micelles solutions by mixing octyl trimethyl ammomium bromide (C_8TAB) and sodium oleate (NaOA). By varying the relative ratio of NaOA to C_8TAB or by fixing the ratio of NaOA to C_8TAB and varying the total surfactant concentration, Raghavan *et al*. [32] were able to produce both linear and branched wormlike micelles. As seen in Figure 4, at a fixed ratio of NaOA/C_8TAB of 70/30, their shear rheology measurements showed a maximum in the shear viscosity at 3wt% while the elastic modulus of the fluids increased monotonically with increasing surfactant concentrations [32,45]. A similar maximum is observed if the total surfactant concentration is held fixed and the relative composition is varied from pure NaOA to pure C_8TAB [32]. Conversely, no maximum is observed in the elastic modulus. The elastic modulus is observed to increase monotonically as $G_0 \propto c^{9/4}$ with

increasing total surfactant concentration. Due to the presence of this maximum in these wormlike micelle systems, solutions with very different compositions can have identical rheological properties in shear. Raghavan *et al*.[32] hypothesized, and later demonstrated through cryo-TEM imaging, that the maximum in the shear viscosity is due to the transition from linear to branched micelles [15,46]. For these systems, branching is achieved by adequately screening the surfactant head groups either through a stoichiometric balance of the oppositely charged surfactant headgroups along the micelle or alternatively through the release of surfactant counterions which results in a reduction of the electrostatic double layer around the micelle [32].

The decrease in the shear viscosity can be attributed to a new stress relief mechanism applicable only to branched micelles. The branch points are not fixed at a specific point along the backbone as is the case for branched polymers, but are free to slide along the micelle resulting in an additional stress relaxation mode not accessible in linear systems [19,47]. The branched points formed in wormlike micelles and their effect on the shear rheology are very different from branched points in polymers which, because they are fixed along the polymer backbone, make movement through reptation more difficult and can dramatically increase the relaxation time and elasticity of the polymeric fluids [22]. Additionally, ghost-like crossings become more likely in systems that favor branches as the energy barrier to produce the temporary branch point decreases.

2.2. Nonlinear Shear Rheology

For many years, the unusual properties of surfactant wormlike micelles have been studied in shear flows of varying geometry. In a steady shear test, wormlike micelles first behave as a Newtonian fluid at low shear rates. As the shear rate is increased, they begin to shear thin. Above a critical shear rate, the shear stress becomes nearly constant and the viscosity decays as $\eta \propto \dot{\gamma}^{-1}$ [48]. This plateau in the shear stress can extend over multiple decades in shear rate before hitting a high shear branch and once again increasing with increasing shear rate. Within this stress plateau, and with proper flow conditions, distinct bands of different shear rate can develop. The physical mechanism leading to the development of these bands has been the subject of intense experimental and theoretical research for the last two decades. Shear bands have been observed using several predominantly optical methods including flow-induced birefringence (FIB) [24,94-51], particle image velocimetry (PIV) [24,52-54], light and small-angle neutron scattering (SANS) [37,55,56], and nuclear magnetic resonance imaging (NMR) [57,58]. An example of a shear-banded flow is shown in Figure 5.

In a given flow, as the shear rate increases to some maximum or critical value, $\dot{\gamma}_M$, the fluid may relax down to the shear stress plateau by forming bands which can coexist at different shear rates. The average of the shear rates from the bands must be that of the applied effective shear rate, where the proportions are described by a simple lever rule [57,58]:

$$\dot{\gamma} = (1-\beta)\,\dot{\gamma}_1 + \beta\,\dot{\gamma}_2 \tag{6}$$

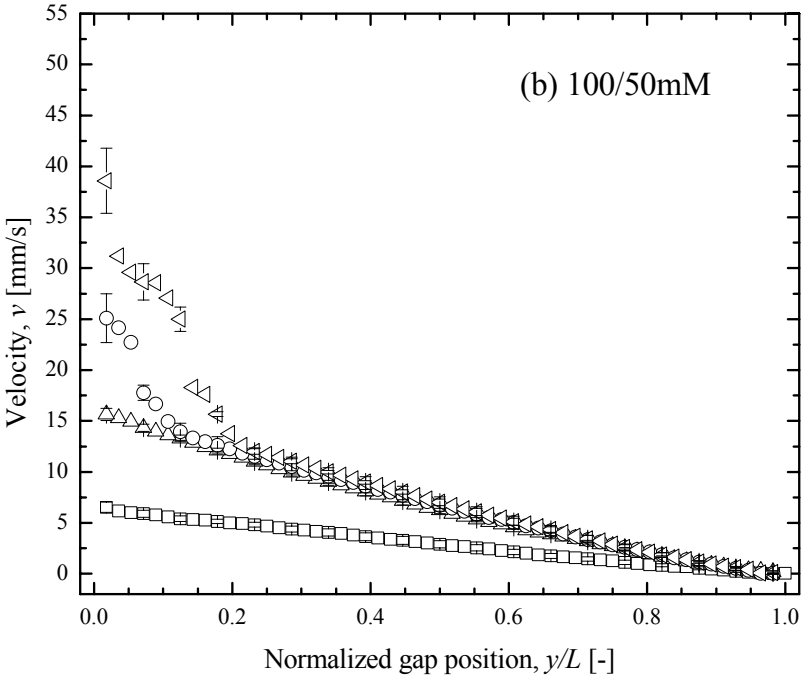

Figure 5: Steady velocity profiles from PIV experiments showing shear band development in a inner-rotating concentric cylinder Couette device with increasing shear rate. The data are for 100/50mM CPyCl/NaSal solutions in 100mM NaCl solution and include shear rates of $\dot{\gamma} = 1\ s^{-1}$ (∀), 3 s^{-1} (8), 6 s^{-1} (–), and 8 s^{-1} (Ξ). The data show the presence of shear bands above $\dot{\gamma} > 3 s^{-1}$. Adapted from Figure 8 of Ref. [24])

As the overall shear rate is increased, the fraction of the high shear rate band, β, is increased as seen in Figure 5. A mechanical rheometer can only measure stress and the nominal shear rate across the entire sample. As a result, rheometry results are observed as the plateau seen in Figure 6 as a dashed line, followed by a transition to the upper shear branch once the stress in the sample is high enough [57].

There is a great deal of research in the area of elucidating the size distribution, and nature of the shear bands that are formed in flows of wormlike micelles. Equation 6 does not give any insight about the size of the bands or even how many bands may exist within the plateau region; it simply constrains the volume fraction in each band [57]. Some numerical calculations and recent experiments [24] seem to suggest two or even three bands, but the size and precise location of these bands is still difficult to predict from theoretical models. The early reptation theory of Doi and Edwards [33] predicts non-monotonic behavior in polymers that become aligned along the flow direction at high shear rates. Later work by Cates and coworkers [28,34,35,59,60]

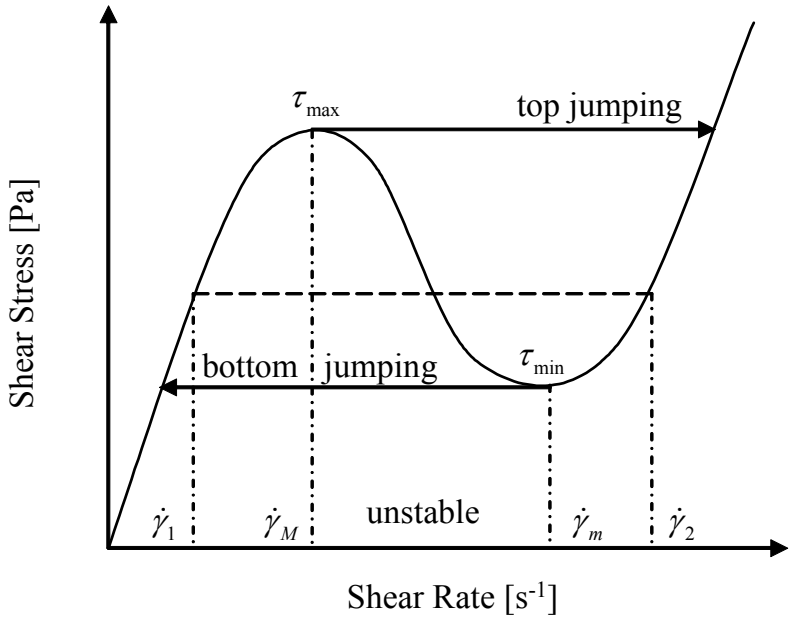

Figure 6: Schematic representation of flow curve exhibiting plateau behavior indicative of shear banding.

extended the Doi and Edwards model to wormlike micelles by incorporating break-up dynamics. The constitutive equations resulting from this analysis allowed good prediction of the observed shear stress in CPyCl/NaSal and other systems [60]. This microscopic constitutive model produces a non-monotonic flow curve, shown in Figure 6 as a solid line. While the plateau, dashed line in Figure 6, is most commonly observed experimentally, some experiments show a hysteretic behavior in controlled stress situations [61]. Top-jumping occurs when the flow curve jumps to the high shear branch directly from $\dot{\gamma}_M$ in an increasing stress experiment, and bottom-jumping when the same flow curve is followed down below the plateau, then jumping to the low shear rate branch from $\dot{\gamma}_m$. The maximum in the shear stress as a function of shear rate can be interpreted as a maximum stress that can be withstood by a reptating micelle tube before it fails [28,35,60]. As the shear rate is increased still further, progressively more tube segments are broken resulting in a decrease in the shear stress. This trend continues until the solvent contribution begins to dominate response of the fluid resulting in an upturn in the shear stress at large shear rates. In the shear rate range between the maximum and minimum in the shear stress, $\dot{\gamma}_M < \dot{\gamma} < \dot{\gamma}_m$, the homogeneous shearing profile is unstable, however, steady flow can be recovered by the formation of shear bands with one band at $\dot{\gamma}_1$ and the other at $\dot{\gamma}_2$ [60,62,63].

While the Cates model furthers our physical understanding of shear banding, because of its numerical complexity, it is only applicable and tractable in simple shear flow calculations. For that reason, a number of macroscopic differential constitutive

models have been studied. The most popular model to use is the Johnson-Segalman model [64] because it exhibits a non-monotonic stress growth with shear rate. Olmsted *et al*. [65,66] later extended this model to include a spatially non-local stress diffusion term that smoothes the interface between the two bands and in doing so sets their location. A similar model, but with variable number density of micelles was considered by Cook and Rossi [67,68]. Among other nonlinear constitutive models, Fischer and Rehage [69] showed that for a number of CTAB/NaSal wormlike micelle solutions that a single-mode Giesekus model [70] with a nonlinear parameter of $\alpha = ½$ (also known as the Leonov model [22]) was able to predict both the linear viscoelastic response and the strong shear-thinning associated with the plateau in the flow curve very well. However, unlike the Johnson-Segalman model, because the Giesekus model does not exhibit a non-monotonic flow curve, it will not produce a shear-banding instability [4]. Still other models use a two-fluid approach that solves separately the force-balance on the solvent and the micelles thereby allowing for variable concentration across the flow [71,72].

The problem with these models is that they are phenomenological by nature. These models simply constitute an average value of stress which has no direct relation to the microstructural dynamics of the wormlike micelles. For the constitutive model to accurately predict the highly non-linear behavior of wormlike micelles recent experiments have shown that it must include local effects on orientation, dynamics, size and concentration of the wormlike micelles [56,58]. The challenge of course is determining how much molecular-level information must be included to reproduce the proper physics while still maintaining a tractable model. A number of groups have begun to develop constitutive models that incorporate the physics of the micellar breakage and reformation processes. Manero and co-workers [73,74] proposed a simple constitutive model based on a codeformational Maxwell model which couples the evolution of the stress to the underlying fluid structure. The model allows for the breakdown of viscoelastic micellar structure under shear into a Newtonian 'fluid' component and the reformation of structure with time. By proposing a break-up rate that is dependent on the local shear rate, this model is capable of producing a non-monotonic flow curve and shear banding. The Manero model quantitatively captures the steady-state and transient shear rheology observed in concentrated cetyltrimethylammonium p-toluenesulfonate (CTAT) solutions. More recently, Vasquez *et al*. [75] proposed a network scission model that is essentially a discretized version of Cates' original reversible break-up theory. In their network model, two micelle species are considered; one of length L that can break in the middle to form two micelles of length $L/2$. The smaller micelles can then subsequently recombine to form a micelle of the original length. In determining the form of the break-up and reformation rates, Vasquez *et al*. followed the work of Tripathi *et al*. [76] who developed a two-species network model for describing the rheology of associative polymers. The VCM model predicts a non-monotonic flow curve and therefore one expects shear banding. In addition, this model is better behaved than the Johnson-Segalman model in that it predicts a maximum in the extensional viscosity as a function of extension rate and obeys the Lodge-Meissner relation in step strain [75]. A recent review by Cates and Fielding [4] goes into great detail about these and other

constitutive models as they apply to wormlike micelle solutions. The interested reader is referred to their work for more information.

In concentrated wormlike micelle solutions, the existence of the non-monotonic shear-banding behavior has been attributed to the formation of highly-aligned nematic states in the high shear band by many researchers [51,53]. Cappelaere *et al*. [77] used both shear- and stress-controlled rheology, along with flow birefringence and small-angle neutron scattering (SANS) to show that a concentrated wormlike system of cetyltrimethylammonium bromide (CTAB) undergoes a first-order isotropic to nematic phase transition induced by shear. In their study, the rheology confirms the stress plateau, flow birefringence allows visualization of the distinct high and low-shear bands, and SANS can provide information about the phase. The work of Berret *et al* [37,48], using highly concentrated solutions of CPyCl/NaSal in sodium chloride (NaCl), provides a great deal of evidence on a phase transition in the wormlike system.

As will be seen in Section 4.6, these phase transitions can also lead to blistering of free interfaces in strong flows. In steady experiments, the CPyCl/NaSal solutions of Berret *et al* in fact show two phases in the high and low shear rate band which are stable, but have differing viscosity, orientation, and order parameters [48]. Transient rheology has further shown that the flow mechanisms for shear-banding are very complex [51]. Observations have shown that there is a first mechanism that occurs on the scale of the fluid's relaxation time, λ, where the micelles behave like a conventional elastic polymers, with a stress overshoot and damped oscillations at higher strain rates. A second mechanism occurs over much longer time scales and manifests itself as a long-time sigmoidal relaxation with a transition from homogeneous to inhomogeneous flow. This behaviour is further evidence of a first-order isotropic to nematic transition which can be accounted for by a simple nucleation and one-dimensional growth model [78].

The stress plateau has also been seen in less concentrated systems, primarily the Rehage and Hoffman model 100mM/60mM CPyCl/NaSal system in water [8,49,52,58,79-81]. These lower concentration systems are far from an isotropic-nematic phase transition on the static phase diagram yet shear banding of the velocity profile as been observed in these systems. Long time transient rheology shows that in terms of stress, the relaxation of a metastable state to a true steady state occurs on a timescale that is much longer than a single Maxwell relaxation time of the fluid [82]. While this behavior is similar to what was reported previously for higher concentration systems [37], where the results are attributed to nucleation and growth of shear-induced nematic phase, it is unlikely that the same is true for solutions at lower weight fractions [82]. The presence of the shear bands is likely the result of a flow-induced shift in the isotropic-nematic phase transition. In addition, Schmidt *et al*. [83] showed that shear-induced phase separation can occur even at relatively low micelle concentrations through a coupling of the concentration and stress profiles. Under shear, regions of an extended micelle will relax quicker in lower concentration and lower viscosity. The micelle thus has a tendency to move from regions of low concentration to high concentration leading to flow-induced demixing and intensification of concentration variations across a flow. Schmidt *et al*. [83] also demonstrated that the concentration variations from the high to the low shear rate band

would result in a stress plateau that was not flat, but had a slight increase with increasing shear rate.

3. EXTENSIONAL RHEOLOGY OF WORMLIKE MICELLE SOLUTIONS

Extensional rheology has recently become a topic of great interest and importance to the complex fluids community. The extensional behavior of polymeric fluids, especially dilute polymer solutions, has received a considerable amount of attention in recent years [84], however, little is known about the behavior of wormlike micelles solutions in extensional flows, in particular transient flows. Devices like the four roll mill and the opposed jet device have been used in the past to investigate the extensional behavior of wormlike micelle solutions [85-92]. Unfortunately, these devices are plagued by an unknown pre-strain history, some degree of shearing in the flow field and the inability to make transient extensional rheology measurements. More recently, the capillary break-up extensional rheometer and the filament stretching rheometer have emerged as accurate devices for reproducibly measuring the response of a wormlike micelle solutions to imposed transient homogeneous uniaxial extensional flow fields [23,38,45,61,93,94]. All of these techniques and the results of the measurements will be described in the section below.

3.1. Opposed Jet Device and Four-Roll Mill Measurements

Prud'homme and Warr [85] were the first to perform a comprehensive study of the extensional rheology of wormlike micelle solutions. They studied a series of equimolar tetradecyltrimethylammonium salicylate (TTABr) and NaSal solutions in both the dilute and semi-dilute regime using a Rheometrics RFX opposed jet device. In this device, two opposed nozzles are immersed in a fluid. Depending on the design, the fluid is then either sucked by a vacuum into the nozzles or pumped through the nozzle to create two impinging jets. The result is an extensional flow field generated in the small gap between the two nozzles [95]. To calculate the extensional viscosity, the force required to maintain the spacing between the two nozzles is measured.

The extensional viscosity of a 25.2mM TTABr/NaSal solution as a function of extension rate is shown in Figure 7. The response of the wormlike micelle solutions studied by Prud'homme and Warr [85] can be best understood within the framework of polymer reptation theory [7]. At Weissenberg numbers below the coil-stretch transition, $Wi = \lambda\dot{\varepsilon} < 1/2$, a plateau in the steady-state extensional viscosity was observed corresponding to the Newtonian response, $\eta_E = 3\eta_0$. Here, $\dot{\varepsilon}$ is the extension rate and λ is the longest relaxation time of the fluid. Unlike entangled polymer melts [96], for which tube orientation has been found to result in extension-rate thinning, no such decrease in the steady state extensional viscosity was observed as the Weissenberg number was increased. At higher extension rates, chain stretching within the oriented segments was observed to lead to extensional thickening of the extensional viscoeity. At a critical Weissenberg number, the extensional viscosity was observed to reach a maximum and decreases with further increases in Weissenberg number. Unfortunately, the data above this critical Weissenberg number is marred by

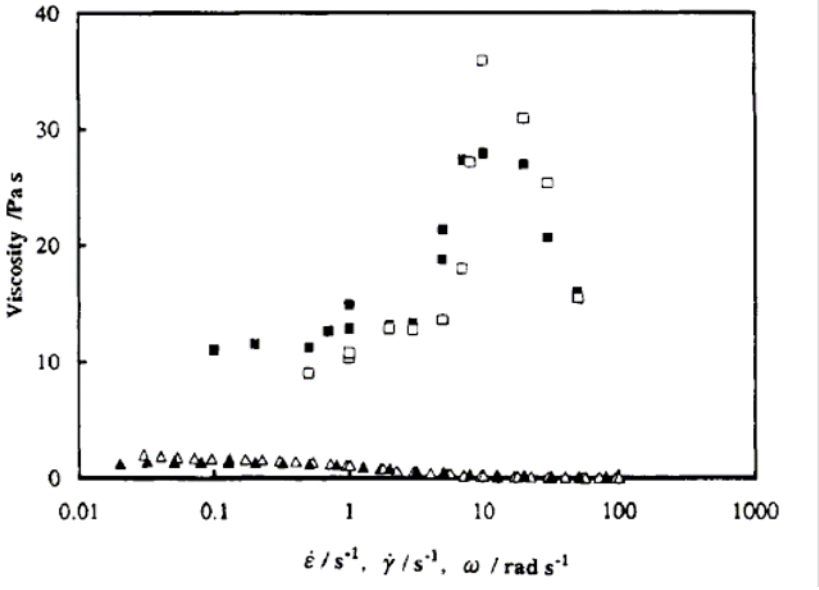

Figure 7: Extensional viscosity as a function of extension rate for a 25.2mM TTABr/NaSal solution. The squares represent two different opposed jet geometries. For comparison, the steady and dyanamic shear viscosities are presented as triangles. Adapted from Figure 4 of Ref. [85])

the onset of a flow instability and the ejection of strongly birefringent fluid from the stagnation region [85]. Even with the problems associated with the stagnation flow field, Prud'homme and Warr [85] theorized that the observed reduction in the extensional viscosity at high extension rates was the result of a scission of the wormlike micelles in the strong extensional flow. The hypothesis of Prud'homme and Warr was later supported by light scattering measurements [86] which clearly demonstrated a decrease in micelle radius of gyration coinciding with the onset of extensional viscosity thinning and the filament stretching experiments of Rothstein [38] which were able to quantify the energy required to scission wormlike micelles in strong extensional flows. These results are in qualitative agreement with the results of Walker *et al*. [89] and Hu *et al*. [97] who showed a similar dependence of extensional viscosity at large extension rates for a series of CPyCl/NaCl and CTAB/NaSal wormlike surfactant solutions respectively in opposed jet devices. Additionally, Walker *et al*. [89] reversed the flow in the opposed jet device to produce a biaxial extensional flow. The results show a marked difference between uniaxial and biaxial extension with little or no extensional thickening observed for biaxial extensional flows of the wormlike micelle solutions. These results suggest that biaxial stretching may be more efficient at disrupting micelles than uniaxial stretching.

In both of these studies, the extensional thickening was not dramatic as Trouton ratios on the order of $Tr = \eta_E / \eta_0 \sim 20 - 40$ were achieved. As a point of reference, a

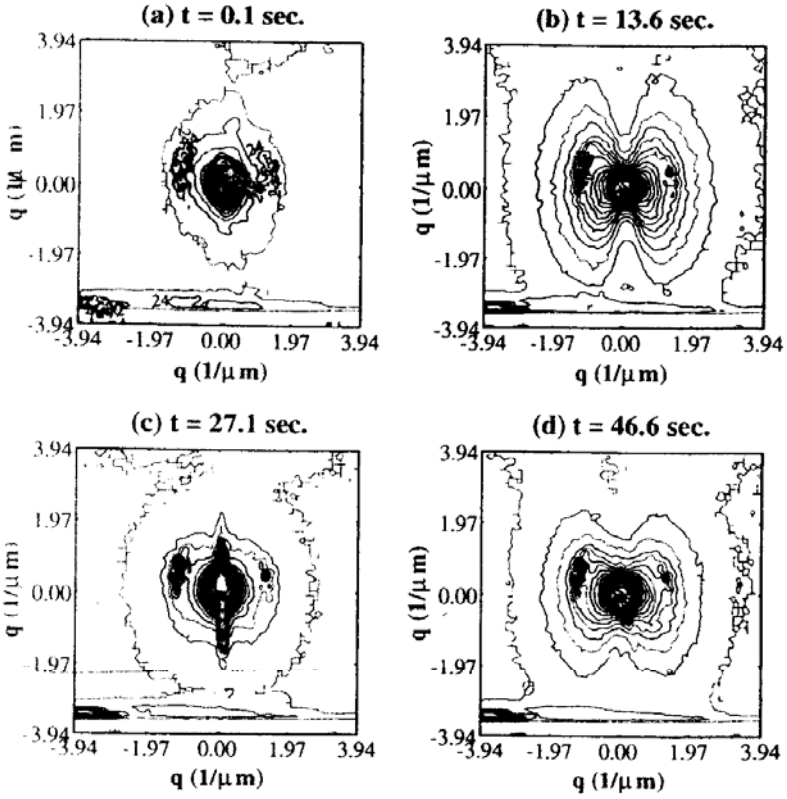

Figure 8: Contour plots of time-dependent SALS patterns for a 30mM CTAB and 230mM NaSal wormlike micelle solution in steady extensional flow with $\dot{\varepsilon} = 1\text{s}^{-1}$ produced by a four-roll mill showing characteristic butterfly patterns in (b) and (d) and a bright streak in (c). Adapted from Figure 10 of Ref. [100])

Newtonian fluid has a Trouton ratio of *Tr* = 3 and dilute polymer solutions have been found to exhibit Trouton ratios in excess of *Tr* > 1,000 [98]. However, it should be noted that the extensional viscosity measured is a strong function of surfactant, salt and temperature. Lin *et al*. [99] used an opposed jet device to measure the extensional viscosity of a number of drag-reducing wormlike micelle solutions. They used a number of oleyl methyl bishydroxyethyl ammonium chloride (O/12) solutions mixed with NaSal at different concentrations and molar ratios. In their study, Trouton ratios exceeding Tr > 500 were found for some samples. A general observation was made that extensional strain hardening decreases with increasing surfactant and salt concentration beyond a molar ratio of 1:1 [99]. These trends were found to be consistent for a number of different surfactant and salt concentrations.

Up to this point we have interpreted the strain hardening results as the stretching of the wormlike micelles. However, there exists another possible explanation. Because the micelles self-assemble and are not covalently bonded like polymer chains, the size of the micelle can shrink or grow depending on the flow conditions. It is therefore possible that the average length of the micelles can increase with flow. Wheeler *et al*. [100] used a Couette cell to produce a shear flow and a four roll mill to produce an extensional flow while simultaneously taking both flow induced birefringence (FIB) and small angle light scattering (SALS) measurements. The advantage of using the four-roll mill is that one gains optical access to the flow. The disadvantage is that a direct measurement of stress cannot be made it can only be inferred from the FIB using the stress-optical rule [90] which unfortunately is only valid at low extension rates and small extensional stresses [38,100]. The SALS measurements of the CTAB/NaSal wormlike micelle solutions that were studied exhibited a butterfly pattern aligned with the flow direction which can be explained as concentration fluctuations linked to hydrodynamic stresses in the fluid. Additionally, as seen in Figure 8, the SALS measurements showed a strong bright streak which fluctuates in time and suggests the formation of an aligned string phase at moderately high shear and extensional rates. Although these observations clearly indicate strong alignment of the wormlike micelles with the flow, it is not clear whether or not these observations also indicate a change in the aggregation number of the wormlike micelles as they unravel, stretch and align with the flow.

3.2. Filament Stretching Extensional Rheometry

Although the techniques described in the previous section are capable of measuring an apparent steady-state extensional viscosity of wormlike micelle solutions, the flow fields are inhomogeneous and plagued by an unknown amount of shear. Additionally, they are not capable or making transient measurements. For high viscosity fluids like polymer melts, there are a number of commercial techniques available such as the Meissner device [101] while for lower viscosity fluids like wormlike micelles, filament stretching extensional rheometers are capable of imposing a transient homogenous extensional flow and measuring extensional viscosity. Filament stretching extensional rheometers are often designed with a long linear stage with two sliding motors designed to impose a homogeneous uniaxial extension on a fluid filament placed between its two endplates. while simultaneously measuring the evolution of the midpoint diameter of the fluid filament created, the force on one of the endplates and the flow-induced birefringence at the midpoint of the fluid filament [84]. A detailed history of the technique can be found in the following papers by the McKinley and Sridhar groups [48,98,102]. The goal of extensional rheometry is to generate a motion profile of the rheometer's endplates such that diameter of the filament is forced to decay exponentially with time and the resulting extension rate imposed on the fluid filament,

$$\dot{\varepsilon} = -\frac{2}{R_{mid}(t)}\frac{dR_{mid}(t)}{dt}, \tag{7}$$

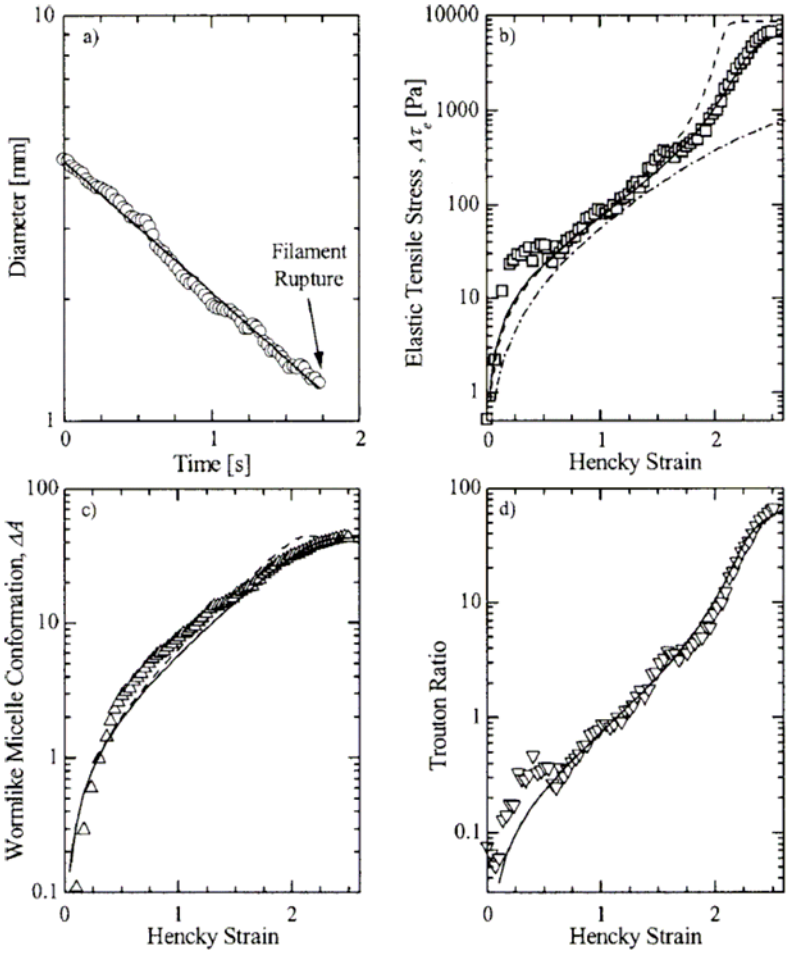

Figure 9: Measurements from a filament stretching experiment of a 50mM CTAB 50mM NaSal wormlike micelle solution at a Weissenberg number of Wi = 8.6. The experiment ends abruptly when the filament ruptures at a Hencky strain of ε_{rupt} = 2.7. Included alongside the experimental data are the predictions of the FENE-PM model, —, the FENE-P model, --, and the Giesekus model, – - –. Adapted from Figure 5 of Ref. [38])

is constant. The deformation imposed upon the fluid filament is often described in terms of a Hencky strain, $\varepsilon = -2\ln\left(R_{mid}/R_0\right)$, where R_0 is the initial midpoint radius of the fluid filament. The elastic tensile stress difference generated within the filament and thus the extensional viscosity of the fluid is calculated from the total force measured by the load cell affixed to one of the rheometer's endplates [103,104].

In the work of Rothstein and coworkers [23,38], a filament stretching rheometer was used to impose a uniaxial extensional flow on a series of CTAB/NaSal and CPyCl/NaSal solutions. Simultaneous measurements of the evolution of the stress and flow induced birefringence (FIB) as a function of time and accumulated strain where made. As seen in Figure 9, these fluids were found to demonstrate considerable strain hardening in the elastic tensile stress and extensional viscosity [38]. Rothstein fit the extensional response of the wormlike micelle solutions with a number of constitutive equations. A good agreement was found between a multimode FENE-P model [105] having a finite extensibility parameter, L^2, determined from the physical model proposed by Shikata *et al*. [25] which is based on rubber elasticity theory and the knowledge of the wormlike micelle structure derived from light scattering. It should be noted that although the steady shear rheology was well fit by a Giesekus model, the large value of the non-linear parameter required to fit the dramatic shear thinning of the shear rheology caused the Giesekus model to severely underpredict the extent of extensional thickening. The development of a constitutive model that is capable of accurately predicting both the shear and extensional rheology of wormlike micelle solutions is still a pressing need and a topic of active research in this field.

Above a critical extension rate, the filament stretching experiments of Rothstein and coworkers [23,38,106] were all observed to come to an abrupt end with the rupture of the fluid filament near its axial midplane. At low Weissenberg numbers, below a critical extension rate, the filaments did not rupture, but instead failed under elasto-capillary thinning. A similar break-up phenomenon was observed by Tripathi *et al*. [76] during filament stretching experiments of a model associative polymer system containing hydrophobically modified ethoxylate-urathane (HEUR) and by Smolka and Belmonte [107] who investigated wormlike micelle solutions in a pendant drop experiment. In the FiSER measurements, the rupture was found to occur at a constant value of the elastic tensile stress, independent of extension rate. As a result, the calculated value of the extensional viscosity was found to decrease with increasing extension rate, $\eta = \Delta\tau_{rupt} / \dot{\varepsilon} \propto \dot{\varepsilon}^{-1}$. The resulting trends in the extensional viscosity are in qualitative agreement with the extensional rheology measurements performed using an opposed-jet device [85,89]. It is likely that observed filament failure and the dramatic downturn in the extensional viscosity measured through opposed-jet devices are related and both likely stem from the scission of wormlike micelles resulting in a dramatic breakdown of the micelle network structure *en masse* [38]. At the point of filament failure, the micelles have been heavily stretched and aligned with the flow. The FIB measurements showed nearly-complete elongation of the wormlike micelle with the anisotropy in the wormlike micelle's conformation exceeding 85% of its finite extensibility parameter in all cases, $\Delta A_f > 0.85 L^2$. Additionally, using the tensile stress at rupture, Rothstein estimated the energy barrier for filament rupture to be roughly $E \approx 4 \mathrm{k_B} T$ independent of salt and surfactant concentration [38] for the CTAB/NaSal solutions.

The dynamics of the filament rupture were captured using a high-speed digital video camera [106] and are shown in Figure 10. Unlike capillary driven filament break-up instabilities, which has been observed to occur in weakly strain hardening fluids after considerable necking of the fluid filament [108], the failure of these

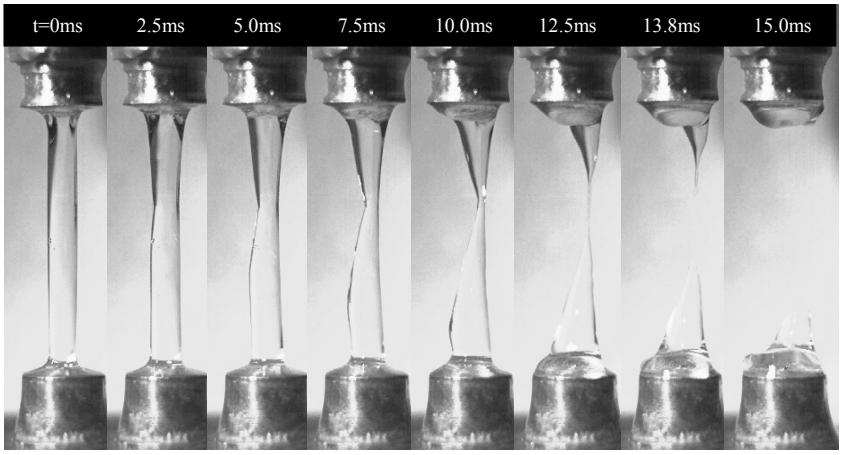

Figure 10: Series of images showing the rupture of a filament of 50mM CTAB 50mM NaSal wormlike micelle solution in a FiSER measurement at a Wi = 8.8. The filament fails at a Hencky strain of ε_f = 2.5. Adapted from Figure 5 of Ref. [106])

wormlike micelle filaments occurs before any significant necking has occurred. The failure appears to be initiated by the growth of a surface or internal defect in the filament that rapidly propagates across the filament cleaving it in two. The propagation of the defect and final failure of the fluid filament is quite rapid, taking less time to complete than the break-up time of the wormlike micelles. A review of the dynamics of the necking of viscoelastic fluid filaments was recently presented by Renardy [109]. In his review, Renardy showed that the purely elastic instabilities that were observed in these filament stretching experiments are independent of surface tension and can occur for fluids in which the extensional viscosity goes through a maximum with increasing strain. The observed filament failure mechanism appears similar to failures observed in tensile loading of elastic solids and extremely elastic polymer melts [110-112]. For the case of elastic solids, samples experiencing a uniform tensile deformation become unstable and fail when the force or the engineering stress goes through a maximum [110]; the Considère criteria [113]. At that point, the solid has exhausted its work-hardening capacity and begun to work-soften, destabilizing any perturbation along the sample and producing a neck that grows rapidly with time.

As we will discuss in the following section, the failure of micelle solutions and associative polymer solutions in uniaxial extensional flows has also been found to lead to new and interesting instabilities in more complex flows such as in the extensional flow in the wake of a sphere falling through a wormlike micelle solution [106,114] or through an associative polymer solution [115] and the extensional flow in the wake of a bubble rising through a wormlike micelle solution [116]. These instabilities have great significance to industrial flows of wormlike micelle solutions such as in turbulent drag reduction where strong extensional flow are often encountered.

3.3. Capillary Break-up Extensional Rheometry

In a capillary break-up extensional rheometer (CaBER), an initial nearly cylindrical fluid sample is placed between the two endplates of the filament stretching rheometer and stretched typically with an exponential profile, $L = L_0 \exp(\dot{\varepsilon}_0 t)$, to a final length of L_f. The stretch is then stopped and the capillary thinning of the liquid bridge formed between the two endplates produces a uniaxial extensional flow that can be used to measure an apparent extensional viscosity [117-122]. One of the advantages of the CaBER technique is that it is capable of measuring the extensional viscosity of fluids with shear viscosities as low as 70mPa·s and relaxation times as low as 10ms [117]. In addition, CaBER can reach extremely large Hencky strains, $\varepsilon > 10$, limited only by the resolution of the diameter measurement transducer.

The break-up of the fluid filament is driven by capillary stresses and resisted by the extensional stresses developed within the flow. The extensional viscosity of the wormlike micelle solution can be determined by measuring the change in the filament diameter as a function of time. Papageorgiou [123] showed that for a Newtonian fluid the radius of the fluid filament will decay linearly with time, $R_{mid}(t) \propto (t_b - t)$. Conversely, Entov and Hinch [121] showed that for an Oldroyd-B fluid, the radius will decay exponentially with time, $R_{mid}(t) \propto \exp(-t/3\lambda_E)$ resulting in a flow with a constant Weissenberg number of Wi = 2/3. This value is larger than the critical Weissenberg number of Wi = 1/2 needed to achieve coil-stretch transition and thus strain hardening of the extensional viscosity of the wormlike micelle solutions can be achieved. Additionally, the slope of the diameter as a function of time can be used to calculate a relaxation time in this elongational flow, λ_E. Theoretical predictions assert that there should be no difference between the relaxation time measured in shear and extensional flow $\lambda_E \approx \lambda$ [121] although this is not necessarily observed in practice. This is likely do to the very rapid and poorly controlled step-strain required to produce the initial fluid filament [124]. An apparent extensional viscosity can be calculated by applying a force balance between capillary stresses and the elastic tensile stresses within the fluid filament [98]

$$\eta_E = \frac{\sigma / R_{mid}(t)}{\dot{\varepsilon}(t)} = \frac{-\sigma}{dD_{mid}/dt}. \tag{8}$$

To calculate the extensional viscosity, the diameter measurements can either be numerically differentiated or fit with the functional form and then differentiated [118].

In Anderson *et al*. [94] and Yesilata *et al*. [61], a capillary break-up extensional rheometer was used to measure the extensional viscosity of erucyl bis(hydroxyethyl)methylammonium chloride (EHAC) and iso-propanol in a brine of ammonium chloride in deionized water. Their results showed a strong extensional hardening for all of the surfactant and salt concentrations that they tested. Additionally, Yesilata *et al*. [61] demonstrated that the extensional relaxation time, λ_E, extracted from intermediate decay of the fluid filament for the EHAC solutions was smaller by a factor of approximately three than the longest relaxation time obtained from oscillatory shear flow measurements, λ. This observation is different from capillary break-up measurements of Boger fluids where the relaxation times were

found to be approximately equal, $\lambda_E \approx \lambda$, as expected from theory [118]. Later CaBER measurements by Bhardwaj *et al*. [23] for a series of CPyCl/NaSal and CTAB/NaSal wormlike micelle solutions showed that the ratio of the extensional relaxation time to the shear relaxation time, λ_E / λ, started at a value much less than one and increased monotonically with increasing surfactant concentration to a value greater than one. Additionally, Miller [125] recently demonstrated that the value of the extensional relaxation time measured was a strong function of the extension rate and total strain imposed on the fluid filament during the initial step-stretch. Finally, if one compares the extensional viscosity measured in CaBER to that in FiSER at nominally the same extension rate, the results do not always agree. Bhardwaj *et al*. [23] showed that for CPyCl/NaSal solutions, the extensional viscosity measurements from FiSER are in some instances more than an order of magnitude larger than those measured using CaBER. These results demonstrate the sensitivity of these self-assembling wormlike micelle solutions to the precise dynamics of the extensional flow and suggest that caution should be used when interpreting CaBER measurements of the extensional viscosity of wormlike micelle solutions and other self-assembling systems.

3.4. Extensional Rheology of Branched Wormlike Micelle Solutions

In extensional flows of linear and long-chain-branched polyolefin melts with similar shear rheology, the branched polymers were found to exhibit significantly more strain hardening in transient extensional flows than the linear polymers [126,127]. The increase in extensional viscosity is a result of increased chain stretching and reptation tube dilation resulting from the relative difficulty associated with moving a branched point in flow. For a branched micelle, the branch point may not represent a similar hindrance to flow. Appell *et al*. [19] hypothesize that sliding of branch points represents a faster stress relief mechanism than reptation or a micelle rupture and reformation process that would allow two micelles to move through each other at an entanglement point. One therefore might expect that when compared to a linear system at the same surfactant concentrations, the extensional rheology of a solution of branched micelles might either exhibit significantly less strain hardening or a delay in the onset of strain hardening to larger extension rates.

Fischer *et al*. [87], studied a series of branched dodecyldimethylamineoxide-sodium laureth sulphate-sodium chloride viscoelastic surfactant solutions. They used an opposed jet device to investigate the effects of wormlike micelle branching in three different samples in an elongational flow. The first sample contains short micelles with no branches, the second sample contains linear, entangled micelles with slight branches, and the third sample contains only branched micelles. The authors conducted a series of experiments for extension rates from $\dot{\varepsilon} = 0.1s^{-1}$ to $20s^{-1}$. The extensional viscosity of the sample containing only short, unentangled micelles did not exhibit any extensional thickening. The authors' second sample which contained linear, entangled micelles showed a very weak maximum of extensional viscosity whereas the third sample which contained branched micelles was found to reach a maximum of extensional viscosity roughly ten times the shear viscosity, $\eta_E^+ \approx 10\eta_0$, followed by extensional thinning with further increases in extension rate. These experiments would suggest that increased branching will result in increases to the extensional viscosity of the wormlike micelle solution. However, one should note that

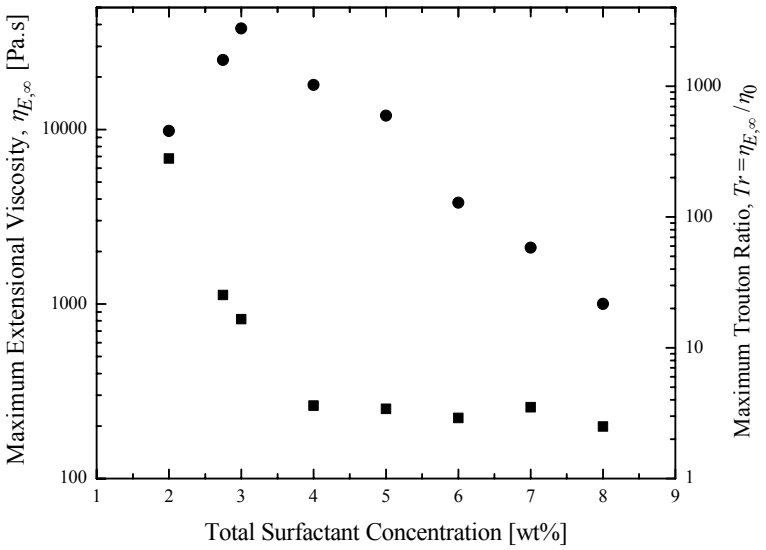

Figure 11: FiSER measurements of the steady-state value of extensional viscosity, ,, and the corresponding Trouton Ratio, !, as a function of total surfactant concentration for wormlike solutions of 70/30 NaOA/C_8TAB in water at a constant Weissenberg number of Wi = 3.2. Adapted from Figure 10 of Ref. [45])

the strain hardening observed by the authors even in the case of the branched system is quite small considering that recent studies of linear wormlike micelle solutions have demonstrated extensional viscosities of more than one thousand times the shear viscosity [23,38,93]. Additionally, although the opposed jet device allows one to measure an apparent extensional viscosity for weakly viscoelastic fluids, it is plagued by an unknown pre-strain history and some degree of shearing in the flow field. It has recently been shown that the extensional rheology of wormlike micelle solutions is extremely sensitive to preconditioning, particularly shear [93].

A systematic study of the role of branching on the extensional rheology of wormlike micelles was performed by Chellamuthu and Rothstein [45] using both a filament stretching extensional rheometer and capillary break-up extensional rheometer. The experiments were performed using a series of linear and branched wormlike micelle solutions consisting of NaOA and C_8TAB having a fixed molar ratio of 70/30 and a total surfactant concentration varied from 2wt% to 8wt%. As seen in Figure 4, the shear rheology of wormlike micelle solutions is found to demonstrate a maximum in shear viscosity at 4wt% followed by a sharp decrease in viscosity with increasing surfactant concentration. Raghavan *et al*. [32] hypothesized, and later demonstrated through cryo-TEM imaging, that the maximum in the shear viscosity is due to the transition from linear to branched micelles [15,46]. As seen in the FiSER measurements presented in Figure 11 and the CaBER measurements reported in [45],

the steady-state value of the extensional viscosity of the wormlike micelle solution was found to demonstrate a similar maximum at 3wt% with increasing total surfactant concentration and increasing degree of micelle branching. Additionally, the steady-state value of the Trouton ratio was found to decay monotonically and rapidly with increasing micelle concentration, approaching an asymptote close to the Newtonian limit for concentrations of 4wt% and above. Although one expects a decrease in the Trouton ratio with increasing concentration and entanglements, the rate of decrease seen in Figure 11 is much faster than what has been observed and predicted for entangled polymer solutions [96]. The authors hypothesized that the dramatic loss of extensional viscosity with the onset of branching was most likely due to the additional stress relief mechanisms available to branched micelles that appear to be extremely efficient in extensional flows. Specifically, the authors cite the fast and fluid sliding of branch points along the length of the micelle and the increased likelihood of 'ghost-like' crossing of micelles at entanglement points with increasing surfactant concentration and the presence of branches. It should be noted that the authors found that the presence of branching did not affect the filament failure mechanism.

The measurements by Chellamuthu and Rothstein [45] suggest that transient extensional rheology measurements can be used to demonstrate a quantitative difference between branched and linear micelles where shear rheology measurements could not. Currently, there are no other mechanical techniques for differentiating a branched micelle solution from a linear entangled micelle solution [128]. Before this work, only cryo-TEM had been successful [14,16-18]. Entangled linear micelles and branched micelles look identical in neutron or light scattering and are difficult to distinguish through measurements of shear rheology or FIB [128].

4. COMPLEX FLOWS OF WORMLIKE MICELLE SOLUTIONS

The ability to characterize the shear and extensional rheology of the wormlike micelle solutions makes it possible to better understand and perhaps even predict the response of these fluids to more complicated flow fields. In the following section we will explore a number of complex flows of wormlike micelle solutions where a wealth of interesting new dynamics have been observed over the last few years and go into some depth into a number of important applications of these materials where the fluids experience strong flows.

4.1. Effect of Pre-shear on Extensional Rheology Measurements

Perhaps the simplest way to study a complex flow is to apply a known pre-shear to a wormlike micelle solution just prior to stretching it in either a FiSER or CaBER. Bhardwaj *et al*. [93] did just that using a number of CTAB/NaSal and CPyCl/NaSal wormlike micelle solutions. As the strength and duration of the applied shear rate were increased prior to a filament stretching experiment, the strain hardening of the extensional viscosity was delayed to larger Hencky strains. This trend is consistent with similar pre-shear measurements for polymer solutions [129], however, it should be noted that the delay is significantly more pronounced for wormlike micelles even at shear rates below a Weissenberg number of $Wi_{shear} < 1$. The

delay in strain hardening likely stems from the need for the micelle to either rotate from the shear direction where it was rotated during the pre-shear cycle into the stretch direction or, alternately, to compress back through its equilibrium conformation before it is subsequently stretched. In the no pre-shear case, the value of the elastic tensile stress at filament rupture was found to be independent of imposed extension rate, however, Bhardwaj *et al*. [93] found that the maximum elastic tensile stress and therefore the extensional viscosity decreased dramatically with increasing pre-shear rate and duration. The most dramatic effects were observed at shear rates for which shear banding had been observed, however, the authors hypothesized that even in the absence of shear banding, the reduction in the strain hardening suggests that the pre-shear might reduce the size of the wormlike micelles or perhaps changes the interconnectivity of the micelle network prior to stretch. This is in stark contrast to the observations of Anna and McKinley [129] who observed no discernable difference in the steady-state value of the extensional viscosity of polymer solutions with and without pre-shear.

Bhardwaj *et al*. [93] also investigated the effect of pre-shear on the extensional viscosity measured in the capillary break-up rheometry experiments. Their observations were very different from that observed in filament stretching. The wormlike micelle solutions were found to strain harden faster, achieve larger steady-state extensional viscosities and an increase in the extensional relaxation time with increasing pre-shear rate and duration. The difference between the response of the wormlike micelles in filament stretching and capillary break-up experiments demonstrates the sensitivity of these self-assembling micelle networks to pre-conditioning and again highlights the difficulty in properly interpreting of CaBER data for wormlike micelle solutions with or without pre-shear. A complete understanding of the response of these wormlike micelle solutions in CaBER may require the development of new constitutive models for wormlike micelle solutions.

4.2. Flow Past a Falling Sphere

The motion of a sphere falling through a viscoelastic fluid is one of the most heavily studied problems in experimental and numerical non-Newtonian fluid mechanics [130-132]. Because of its geometric simplicity and the complex nature of the flow with regions of shear near the sphere and extension in the wake, the motion of a sphere falling in a bounded cylinder of fluid has been chosen as a benchmark problem for numerical simulations [133]. This flow is thus an excellent choice for experimentally investigating the response of wormlike micelles to complex flows as was done by both Jayaraman *et al*. [114] and Chen and Rothstein [106] using CTAB/NaSal solutions of different concentrations.

In Chen and Rothstein [106], a detailed experimental investigation of the flow of a 50mM CTAB and 50mM NaSal wormlike micelle solution past a falling sphere falling within a column of a wormlike micelle solution was presented. By determining the terminal velocity of a number of different density spheres, the drag was calculated as a function of Weissenberg number. At low Weissenberg numbers, the drag on the spheres was near the expected Newtonian limit. As the Weissenberg number was increased, the drag was observed to decrease as a result of shear thinning. As the

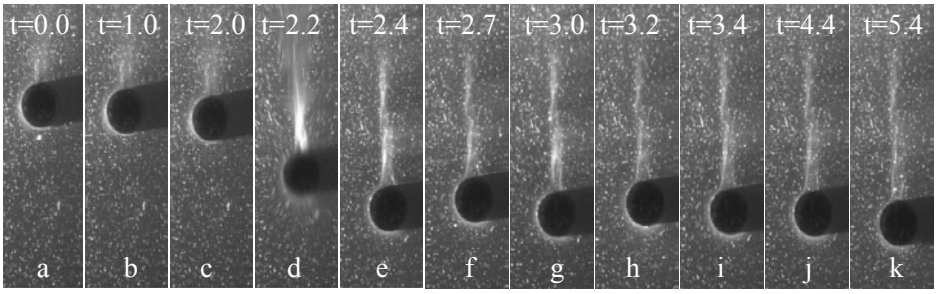

Figure 12: A series of images showing the unstable motion of an aluminum oxide sphere with a sphere-to-tube ratio of a/R = 0.125 and falling with an Weissenberg number of Wi = 3.8. (Adapted from Figure 8 of Ref. [106])

Weissenberg number was increased further, the establishment of a strong extensional flow in the wake of the sphere causes the drag to increase to a value larger than that of a Newtonian fluid with the same viscosity. The presence of the strong extensional flow was documented through both full field and pointwise FIB measurements and resulted in a strong negative wake behind the sphere.

At a critical Weissenberg number, the flow becomes unstable and fluctuations in the sedimentation velocity of the sphere are observed. A series of images are presented in Figure 12 documenting the unstable sedimentation of an aluminium oxide sphere. For the unstable flows, the velocity flow field is observed to fluctuate between a negative and extended wake while the FIB measurements demonstrated a time-periodic growth and pinch-off of a strong birefringent tail in the wake of the sphere. Jayaraman *et al*. [114] also observed an instability in the sedimentation velocity of a sphere falling through a 9mM CTAB an 9mM NaSal wormlike micelle solution. With the exception of the measurements of Bisgaard [134] which showed a fluctuating velocity in the wake of a sphere falling through a polyacrylamide solution at high Weissenberg number that was never independently reproduced, no other low-Reynolds number elastic flow instabilities have been observed for a sphere falling through a polymer solution or melt. The instability observed by Jayaraman *et al*. [114] and Chen and Rothstein [106] is most likely a stress-induced evolution of the entangled wormlike micelle network structure. Chen and Rothstein [106] presented strong FIB evidence that suggests that the flow instability is the result of a breakdown of the wormlike micelle network structure in the wake of the sphere. This breakdown is shown to be related to the filament rupture observed in the extensional rheology experiments [38].

4.3. Flow Past a Rising Bubble

An interesting parallel experiment to the flow past a falling sphere is the flow past a rising bubble. The geometry is quite similar in both experiments, except in the case of a rising bubble, the interface is no longer no-slip nor is it non-deformable. In a number of interesting experiments, Liu *et al*. [135] studied rising bubbles in

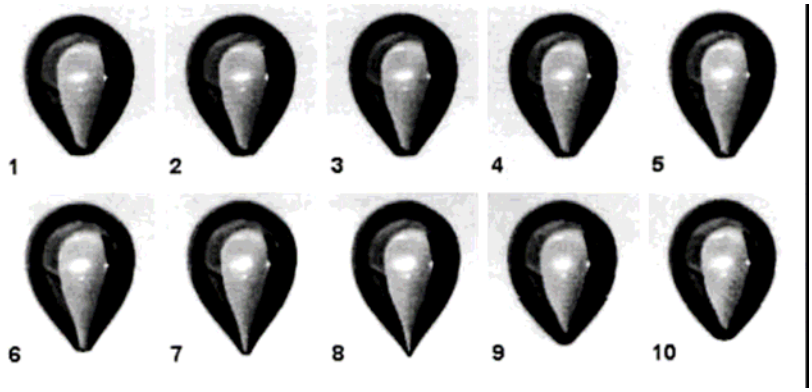

Figure 13: A series of images taken 67ms apart showing the unstable motion and oscillating cusp of an air bubble rising through an 10.7mM CTAB and 10.7mM NaSal wormlike micelle solution. (Adapted from Figure 3 of Ref. [136])

viscoelastic polymer solutions. They demonstrated that at flow rates corresponding to large capillary numbers, a two-dimensional cusp or a "knife's edge" which is sharp in one direction and broad along an orthogonal view can appear at the tail of the rising bubble while the leading edge remains approximately spherical.

The motion and shape of a rising bubble in polymer solutions has been found to be stable. However, a new instability was discovered for the flow of a both CTAB/NaSal and CPyCl/NaSal solutions past a rising air bubble by Belmonte and coworkers [116,136]. As seen in Figure 13, above a critical velocity, the tail of the bubble was found to grow slowly with time until it reached a maximum length at which point the tail was observed to retract quickly and then begin to grow again with time. The sudden retraction of the tail was observed to correlate with a rapid acceleration of the bubble. Handzy and Belmonte [116] demonstrated that the nature and presence of the instability was directly related to the wormlike micelle concentration and possibly the presence of branching in the wormlike micelles. The presence of the surfactant is most likely not the cause of the oscillations because there exist a number of concentration and temperature regimes where the cusps do not oscillate and are stable. Additionally, as with the sedimentation of the spheres, FIB measurements have shown that a strong extensional flow is present in the wake of the rising bubble. The origins of this instability is therefore likely the result of a breakdown of wormlike micelles in the wake of the bubble and related to the unstable motion of spheres [106,114] and the rupture of fluid filaments in extensional flows [23,38,107]. However, so that the reader doesn't think that wormlike micelle solutions have cornered the market on interesting flow phenomena in the wake of bubbles, Soto *et al*. [137] observed some fascinating flow structures including a long tail in the wake of a bubble rising through an associative polymer solution. As with wormlike micelle solutions, these interesting flow phenomena are the result of the coupling of

microstructure of the associative polymers with the stresses fields and flow kinematics.

4.4. Flow through Porous Media

Understanding the flow of viscoelastic wormlike micelle solutions through porous media has become an extremely important industrial problem because wormlike micelle solutions are finding use in enhanced oil recovery where they are often used as a polymer-free fracture fluid for stimulating oil production [1,20,138,139]. Fracture fluids are driven into recovery wells at enormous pressure in order to open up cracks in the sandstone and speed up oil recovery. Wormlike micelle solutions are ideal for these applications because they shear thin extremely quickly which allows them to be pumped relatively easily and at low cost. Additionally, the high zero-shear viscosity of the fracture fluids allows sand or other proppants to be suspended in the fluid and transported to the newly induced fracture under pressure where they pack tightly enough to keep the fracture from fully closing when the well is depressurized yet with enough permeability to maintain efficient flow. The recent turn to wormlike micelle solutions as fracture fluids as a replacement for polymer solutions is due to a number of advantages that they possess. In order to transport the proppants into the fractures, the fluid's viscosity has to be very high. In the case of polymer solutions, large viscosities are typically achieved using high concentrations of high molecular weight polymers, which are often cross-linked into gels [20,138]. Once the proppants are in place, the fluid must lose its viscosity to allow the proppants to settle into place and the carrier fluid to be flushed out of the well. For polymer gels, the solution is the use of delayed oxidization or enzymes to break down the polymers; a process which is often inefficient. On the other hand, the morphology of micelles changes from wormlike to spherical upon contact with oil in the reservoir resulting in orders of magnitude reduction in the fluid's viscosity and nearly complete recovery of the fracture fluid from the reservoir [20,138]. Wormlike micelle solutions have found use in a number of other oilfield applications as well. For a more complete and detailed review, the readers are directed to the papers by Maitland [138] and Kefi *et al*. [20].

The flow through porous media is a tortuous flow with regions of high shear in cracks and narrow capillaries and regions of strong extensional flow as the fluid is accelerated into capillaries from relatively large reservoirs or holes within the rock. Unfortunately, flow through cores of sandstone or other opaque porous media it is difficult to analyze because the exact nature of the media is unknown and the flow cannot be visualized. For that reason, most porous media studies use an idealized porous media like a packed bed of glass spheres where the permeability and tortuosity are known a priori and the flow can be observed to some extent with proper index of refraction matching [92,140].

For Newtonian fluids in porous media, the flow can be described using Darcy's law which states that the average velocity through the media can be determined from $\bar{V} = \phi \Delta p / \mu$, where ϕ is the porosity of the media, Δp is the pressure drop and μ is the Newtonian viscosity [131]. Clearly, when the fluid is viscoelastic, Darcy's law is not

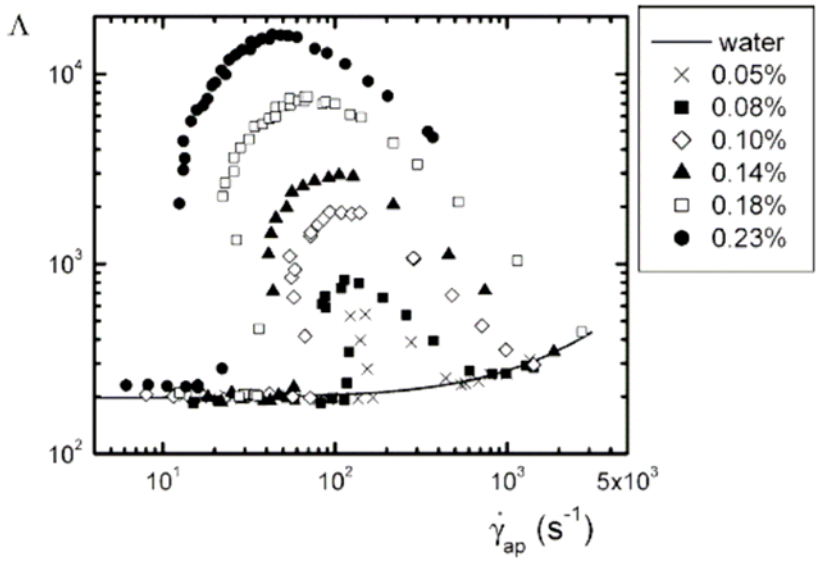

Figure 14: Flow of CTAT solutions through an idealized porous media. The figure is plotted in terms of a resistance coefficient, Λ, as a function of shear rate. (Adapted from Figure 4 of Ref. [92])

sufficient to describe the flow rate as a function of pressure drop. Often, an effective Darcy's viscosity or a resistance coefficient, $\Lambda = \mu_{app}/\mu$, are measured experimentally or derived through numerical simulations as a function of flow rate for viscoelastic fluids so that Darcy's law can continue to be used. For the case of the flow through a packed bed of spheres of diameter d as seen in Figure 14 the dimensionless apparent viscosity becomes

$$\Lambda = \frac{d^2\phi^3(\Delta P/L)}{\mu\bar{V}(1-\phi)^2}, \tag{9}$$

and the effective shear rate is approximated by $\dot{\gamma}_{app} = 20\bar{V}/\phi d$ [92]. For polymers like polyacrylamide (PAA) which strain harden in extensional flows and shear thin in shear flows, extremely large Darcy viscosities have been measured demonstrating how dominant the extensional component of porous media can be to the overall flow [140,141]. Similar observations were also made for wormlike micelle solutions [92,142]. Muller *et al*. [92] investigated the flow of a CTAT solution through a packed bed of monodisperse 1mm glass spheres. The shear rheology of the CTAT showed a modest shear thickening while the opposed-jet measurements of the extensional viscosity showed very little if any strain hardening. Although, it should be noted that the lack of strain hardening might simply be a result of scission of the wormlike micelles at the very large extension rates applied. As seen in Figure 13, for relatively low CTAT concentrations, the resistance coefficient was found to increase quite dramatically with increasing shear rate. The increase is an order of magnitude larger

than the shear thickening observed which the authors hypothesize is a synergistic interaction between the shear and extensional components of this complex flow resulting in the large observed viscosity enhancement [92]. Similar behaviour was observed even for the most dilute solutions that the authors explored even those not demonstrating shear thickening. Recently, Boek *et al.* [143] experimentally investigated the flow of EHAC through a microfluidic expansion contraction. Micro particle image velocimetry (μ-PIV) measurements of the flow through this idealized pore showed large recirculation regions upstream of the contraction. As has been seen with similar flows of polymer solutions [144,145], these vortices appeared to be unstable thus demonstrating how complex the flow through the pore space in natural rock can be. With the importance of the flow of wormlike micelle solutions through porous media one would expect there to be more literature available than there is. Clearly, this is an area where fundamental studies with well-characterized fluids can still have a major impact on an extremely important and continuously evolving industrial field.

4.5. Turbulent Drag Reduction

It has been known for quite some time that the addition of high molecular weight polymers or wormlike micelles to high Reynolds number turbulent flows can produce significant turbulent drag reduction [2,146]. A significant effort has been made recently to understand polymer drag reduction. Direct Numerical Simulations (DNS) coupled with constitutive models such as the FENE-P [147-150] or Giesekus model [148] or with Brownian dynamics simulations of the polymer deformation using FENE dumbbells [151] have helped to explain the origins of polymer drag reduction. These simulations clearly demonstrate that polymer solutions with large ratios of their extensional to shear viscosity (large Trouton ratios) inhibit turbulent generation events within the buffer layer where polymers are stretched near their finite extensibility limit by strong biaxial extensional flows [148]. Additionally, energy spectrum analysis has shown that a substantial fraction of the energy produced by the mean flow is transferred into elastic potential energy of the polymers [149] around near-wall vortices [150] thereby reducing the intensity of turbulent fluctuations. The energy stored in the polymer is subsequently returned to the flow as the polymer relaxes and can increase energy of streamwise fluctuations and streaks even as near wall turbulence is damped [149,150].

An excellent review on surfactant-induced drag reduction was written by Zakin *et al*. [2] about ten years ago. Since the publication of that review, Zakin and coworkers have undertaken an extensive experimental investigation to understand the impact of wormlike micelle structure and rheological properties on drag reduction. Their studies included an investigation of the influence of type and quantity of counterion in cationic systems [99,152,153] and the effect of various mixtures of cationic and zwitterionic surfactants [154,155]. The authors conclude that the only clear prerequisite for drag reduction appears to be the presence of wormlike micelles and the subsequent strain hardening of the extensional viscosity. This is consistent with the analysis of polymer-induced turbulent drag reduction. For polymer drag reduction, a maximum drag reduction asymptote (MDRA) exists which limits the extent of drag reduction that can be achieved [146]. A similar MDRA exists for

surfactant drag reduction, however, even though the drag reduction mechanism appears to be the same for polymers and wormlike micelles, the MDRA for surfactant drag reducers has been found to be between 5-15% higher depending on Reynolds number [156,157]. This is even more remarkable when one considers that the zero-shear rate viscosity of the drag-reducing wormlike micelle solutions are often an order of magnitude larger than that the drag-reducing polymer solutions and water. It still remains an open question why surfactant solutions are so much more efficient at reducing turbulent drag. It is possible that the difference is linked to the additional energy dissipated by wormlike micelles as they break down under strong stretching flows. However, we won't know for certain until tractable constitutive models for wormlike micelles have been developed and large-scale DNS simulations can be performed with them.

4.6. Impact of Drops and Spheres

Understanding the impact dynamics of droplets of wormlike micelle solutions on dry surfaces as well as thin films of viscoelastic wormlike micelle solutions is important to applications ranging from inkjet printing to agrochemical spraying to spray coating where viscoelastic additives are often used to reduce secondary drop formation and the rebound of the impinging drop. A number of experiments have also been performed studying the effect of dynamic surface tension and elasticity on the impact of dilute polymer solutions and surfactant solutions on dry surfaces [158-161]. These studies demonstrated that the addition of a small amount of polymer solution or wormlike micelles dramatically increases the threshold for splashing and drop rebounding. These studies found that the drop impact dynamics are a strong function of the surface hydrophobicity and roughness, the Ohnesorge number, the Webber number and the Weissenberg number of impact. Similar measurements were done for the impact of drops on thin films of wormlike micelle solutions [162]. The addition of elasticity to the thin film fluid was found to suppress the crown growth and the formation of satellite drops with the largest effects observed at small film thicknesses. Similar observations were made for the impact of drops on thin films of polymer solutions [163]. In contrast to polymer solutions where the height of the Worthington jet was found to increase monotonically with increasing drop velocity [163], a plateau was found in the growth of the maximum height of the Worthington jet with increasing impact velocity for a series of wormlike micelle solutions [162]. Lampe *et al*. [162] hypothesized that the complex behavior of the Worthington jet growth was the result of a dissipative mechanism stemming from the scission of wormlike micelles under the strong extensional and shear flow conditions.

The impact of solid spheres on deep reservoirs of polymer solutions and wormlike micelle solutions was recently investigated. Cheny and Walters [163] showed that the large extensional viscosities of polymer solutions resulted in a significant reduction in the maximum height reached by the Worthington jet upon impact. Additionally, the viscoelasticity has been found to cause spheres to oscillate before coming to steady-state velocity after being released from rest within the fluid [164] or being dropped from a height above the surface of the fluid [165]. Akers and Belmonte [165] made a number of interesting observations while studying the impact of spheres on an 80mM CPyCl 60mM NaSal wormlike micelle solution. They found

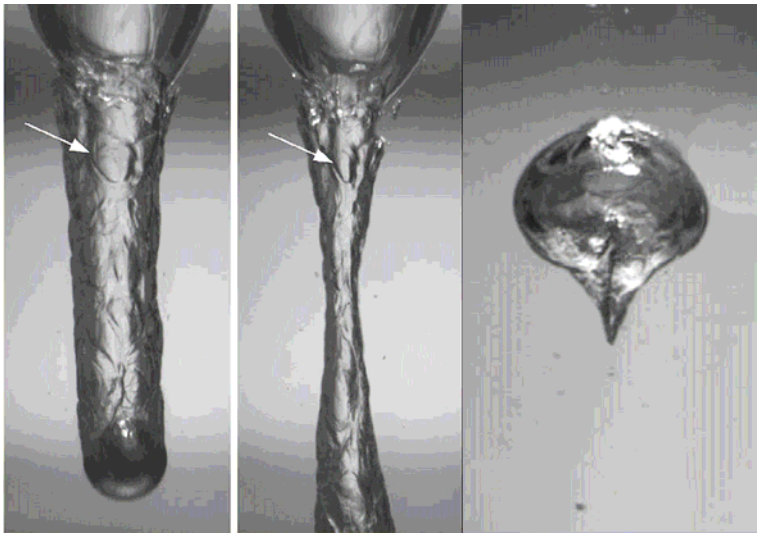

Figure 15: Impact of a 0.95cm steel sphere dropped from 70cm on an 80mM CPyCl 60mM NaSal wormlike micelle solution. The images show the formation of texture on the surface of the cavity that does not stretch or move as the sphere falls through the fluid. The texture is also observed for large ($2cm^3$) bubbles rising through the wake of the sphere. (Adapted from Figures 11 and 15 of Ref. [165])

that above a critical impact velocity, the air cavity formed behind the impacting sphere transitions from a smooth interface and pinch-off as has been previously observed for impacts on both Newtonian fluids and polymer solutions to a heavily textured surface shown in Figure 15. The authors suggest that the irregularities at the air-fluid interface may be the result of localized fracture of the wormlike micelles as they are stretched by the impacting sphere. Similar blistering has been observed on filaments of wormlike micelles being stretched just prior to filament rupture [107] and can also be observed at the interface of large bubbles rising through the wake of falling sphere as seen in Figure 15 [165]. Additionally, these bubbles are observed to take on an odd, spade-like or inverted heart shape as they rise. Zhou *et al*. [166] recently showed that by modelling the fluid in the wake of the sphere as an aligned nematic phase with an anchoring energy on the bubble that is of the same order as the interfacial tension and the bulk elasticity of the fluid, that the shape of the bubble could be qualitatively predicted numerically.

4.7. Atomization and Sprays

The structure, kinematics and stability of thin films has been well studied both experimentally and analytically throughout the literature for Newtonian fluids [167-170]. However, despite the importance of these fluids and flows to a host of commercial and industrial applications such as agrochemical spraying, spray coating, and inkjet printing, little work has been done to study the break-up of thin films of

viscoelastic fluids [171-177]. By comparison, the break-up of viscoelastic fluid jets is well understood and it has been shown that strain hardening of the extensional viscosity can stabilize viscoelastic jets while retarding satellite drop formation and increasing the main droplet size [61,178-181]. A number of experimental studies of the atomization of polymer solutions have found that the addition of viscoelasticity and specifically large extensional viscosities negatively impact atomization of thin films formed by a number of different types of nozzles because viscoelasticity tends to stabilizes both the external rim of the thin films and the internal rims formed as the thin film ruptures [171,172,174]. Additionally, it has been demonstrated that increasing extensional viscosity increased the average size of the spray droplets and broadened the drop size distribution [171,172]. These studies clearly demonstrate that the rheology of the fluid must be strongly considered when choosing or designing a nozzle to atomize viscoelastic fluids.

Brenn *et al*. [176] performed a linear stability analysis on an infinitely wide non-Newtonian liquid sheet moving within an inviscid gas. They showed that unlike a liquid jet, for a liquid film surface tension is stabilizing and not destabilizing. The sheets are instead primarily destabilized by aerodynamic effects. The fluid viscosity also stabilizes the sheets, but the elasticity of the non-Newtonian fluid strongly destabilizes the sheet increasing the growth rates of both symmetric and anti-symmetric two and three-dimensional disturbances [176]. These predictions may seem to contradict the experimental observations; however, Brenn *et al*. [176] did not consider the rim of the fluid sheet in their analysis so to understand their results one must focus only on the change of stability of the internal sheet and not its rim. These predictions were recently supported by a number of experiments performed using a series of CTAB/NaSal wormlike micelle solutions designed to investigate the flow kinematics and stability of viscoelastic fluid sheets produced from a series of commercially available flat-fan and hollow-cone spray nozzles [175,177]. As the flow rate through the nozzles was increased, the viscoelastic fluid sheets were found to grow larger; eventually becoming unstable, and atomizing into drops. For the flat-fan spray-nozzles, Newtonian water sheets were found to first destabilize along the fluid rim. The addition of viscoelasticity was found to stabilize the rim while simultaneously destabilizing the fluid sheet in agreement with the predictions of Brenn *et al*. [176]. The internal rims seen in Figure 16 were produced by multiple holes in the sheet eventually colliding to produce a complicated highly interconnected structure which is similar to the ‘fluid webs’ observed by Miller *et al* [175]. Both the rim at the edge of the fluid sheet and the internal rims are long-lived owing to the large extensional viscosity of the fluid thereby reducing the efficiency of atomization. Additionally, it is the lack of a rim along the fluid sheets produced by a hollow-cone nozzle that appear to result in an improved atomization for viscoelastic fluids [177]. Increasing viscoelasticity of the test fluid was found to stabilize the thin films produced by both the flat-fan and hollow-cone spray nozzles, thereby shifting the break-up of the sheets to larger flow rates. However, beyond the critical flow rate for sheet rupture, increases to the fluid elasticity were found to alter the dynamics of the atomization of the viscoelastic fluid sheets by increasing the number and growth rate of holes in the sheet while simultaneously reducing the initiation time for sheet

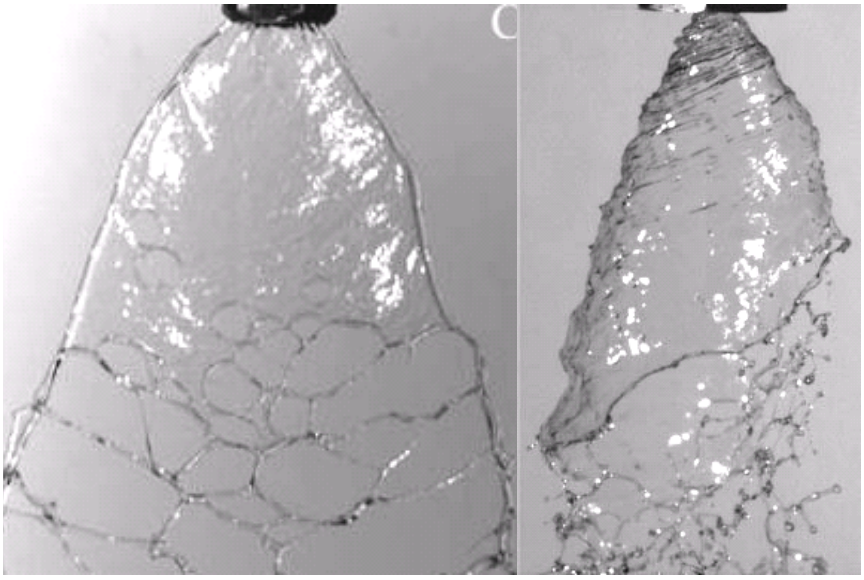

Figure 16: The break-up of sheets of 10mM CTAB/NaSal produced by a 65^{o} flat fan nozzle and a hollow-cone nozzle at Webber numbers $We = 1.1\times10^{4}$ and $We = 2.9\times10^{3}$ respectively. (Adapted from Figures 8 and 17 of Ref. [177])

rupture. It is not yet known whether these observations are general for viscoelastic fluids or unique to wormlike micelle solutions.

5. CONCLUSIONS

In this review, we have surveyed recent experimental, numerical and theoretical developments for nonlinear rheology of viscoelastic wormlike micelle solutions and the response of these complex fluids to strong flows. Specific emphasis was placed on extensional rheology measurements and complex flows having strong extensional components where a wealth of interesting new flow phenomena have recently been discovered. In many of these flows, viscoelastic wormlike micelle solutions behave in a manner very similar to polymer solutions. Wormlike micelle solutions demonstrate strain hardening of their extensional viscosity that can result in an increased resistance to complex flows such as the flow past a sphere or the flow through porous media. Additionally, the large extensional viscosity of these fluids has led to significant drag reduction in turbulent flows. However, wormlike micelles are self-assembled and as such are quite different from polymer solutions. Under large elastic stresses, wormlike micelles can break apart. This failure and the resulting morphological changes have been linked to a number of newly discovered elastic instabilities not present in polymer solutions.

In each of the previous sections, we have attempted to note some specific challenges and open questions that remain in this relatively new and exciting research field. Just as the amazing complexity of wormlike micelle solutions makes them so fascinating to work with, it is this same complexity that makes the response of these fluids difficult to understand, to interpret and ultimately to predict. Experimental results of wormlike micelle solutions in strong flows are becoming more and more plentiful; however, currently our interpretation of these results are performed with only a partial understanding of the underlying micelle dynamics in strong flows. An in-depth understanding of the underlying physics can only be achieved through systematic studies which directly compare careful experimental measurements and the predictions of constitutive models derived explicitly for wormlike micelle solutions. Phenomenological models such as the Johnson-Segalman model are not sufficient because they simply constitute an average value of stress which has no direct relation to the microstructural dynamics of the wormlike micelles. Constitutive models must be developed which include local effects on orientation, dynamics, size and concentration of the wormlike micelles. The challenge of course is determining how much molecular-level information must be included to reproduce the proper physics while still maintaining a tractable model. It is encouraging that a number of groups have taken up this challenge and have begun to develop constitutive models that incorporate the physics of the micellar breakage and reformation processes. I look forward to seeing what the next few years will hold.

ACKNOWLEDGMENTS

The author would like to express his sincere thanks to both his current and former students whose work constituted a large part of this review article. The author would also like to thank the National Science Foundation for financial support.

REFERENCES

1. Anderson, V J, Pearson, J R A and Boek, E S, *The Rheology of Worm-Like Micellar Fluids*, in *Rheology Reviews*, D.M. Binding and K. Walters, Editors. 2006, The British Society of Rheology. p. 217-253.
2. Zakin, J L, Lu, B and Bewerdorff, N W, *Surfactant drag reduction.* Rev. Chem. Eng., 14(45) (1998) 253-320.
3. Dreiss, C A, *Wormlike micelles: where do we stand? Recent developments, linear rheology and scattering techniques.* Soft Matter, 3 (2007) 956-970.
4. Cates, M E and Fielding, S M, *Rheology of giant micelles.* Adv. Phys., 55(7-8) (2006) 799-879.
5. Yang, J, *Viscoelastic wormlike micelles and their applications.* Current Opinion in Colloid and Interface Sci., 7 (2002) 276-281.
6. Israelachvili, J N, *Intermolecular and surface forces: with applications to colloidal and biological systems*. Academic Press (London) (1985). 296.

7. Larson, R G, *The Structure and Rheology of Complex Fluids*. Oxford University Press (New York) (1999). 364.
8. Rehage, H and Hoffmann, H, *Viscoelastic surfactant solutions: model systems for rheological research.* Mol. Phys., 74(5) (1991) 933-973.
9. Schurtenberger, P, Scartazzini, R, Magid, L J, Leser, M E and Luisi, P l, *Structural and dynamic properties of polymer-like reverse micelles* J. Phys. Chem., 94(9) (1990) 3695-3701.
10. Tung, S-H, Huang, Y-E and Raghavan, S R, *A new reverse wormlike micellar system: Mixtures of bile salt and lecithin in organic liquids.* J. Am. Chem. Soc., 128 (2006) 5751-5756.
11. Laughlin, R G, *The Aqueous Phase Behavior of Surfactants*. Academic Press (New York) (1994).
12. Israelachvili, J N, *Intermolecular and surface forces*. 2nd ed. Academic Press (London ; San Diego) (1992). xxi, 450.
13. Lequeux, F and Candau, S J, *Structural Properties of Wormlike Micelles*, in *Theoretical Challenges in the Dynamics of Complex Fluids*, T. McLeish, Editor. 1997, Kluwer Academic Publishers: Netherlands. p. 181-190.
14. Danino, D, Bernheim-Groswasser, A and Talmon, Y, *Digital cryogenic transmission electron microscopy: an advanced tool for direct imaging of complex fluids.* Colloids and Surfaces A: Physicochemical and Engineering Aspects, 183 (2001) 113-122.
15. Cui, H, Hodgdon, T K, Kaler, E W, Abezgauz, L, Danino, D, Lubovsky, M, Talmon, Y and Pochan, D J, *Elucidating the assembled structure of amphiphiles in solution via cryogenic transmission electron microscopy.* Soft Matter, 3 (2007) 945 - 955.
16. Danino, D, Talmon, Y, Levy, H, Beinert, G and Zana, R, *Branched threadlike micelles in an aqueous solution of a trimeric surfactant.* Science, 269 (1995) 1420-1421.
17. Danino, D, Talmon, Y and Zana, R, *Alkanediyl-alpha,omega-bis(dimethylalkylammonium bromide) surfactants (dimeric surfactants). 5. Aggregation and microstructure in aqueous solutions.* Langmuir, 11 (1995) 1448-1456.
18. Danino, D, Talmon, Y and Zana, R, *Cryo-TEM of thread-like micelles: on-the-grid microstructural transformations induced during specimen preparation.* Colloids and Surfaces A: Physiochemical and Engineering Aspects, 169 (2000) 67-73.
19. Appell, J, Porte, G, Khatory, A, Kern, F and Candau, S J, *Static and dynamic properties of a network of wormlike surfactant micelles (etylpyridinium chlorate in sodium chlorate brine).* J. Phys. II, 2 (1992) 1045-1052.
20. Kefi, S, Lee, J, Pope, T, Sullivan, P, Nelson, E, Hernandez, A, Olsen, T, Parlar, M, Powers, B, Roy, A, Wilson, A and Twynam, A, *Expanding applications for viscoelastic surfactants.* Oilfield Review, (2004) 10-16.
21. Rehage, H and Hoffmann, H, *Rheological Properties of Viscoelastic Surfactant Systems.* J. of Phys. Chem., 92 (1988) 4712-4719.

22. Bird, R B, Armstrong, R C and Hassager, O, *Dynamics of Polymeric Liquids: Volume 1 Fluid Mechanics*. John Wiley & Sons (New York) (1987).
23. Bhardwaj, A, Miller, E and Rothstein, J P, *Filament stretching and capillary breakup extensional rheometry measurements of viscoelastic wormlike micelle solutions.* J. Rheol., 51(4) (2007) 693-719.
24. Miller, E and Rothstein, J P, *Transient evolution of shear banding in wormlike micelle solutions.* J. Non-Newtonian Fluid Mech., 143(1) (2007) 22-37.
25. Shikata, T, Dahman, S J and Pearson, D S, *Rheo-optic behavior of wormlike micelles.* Langmuir, 10 (1994) 3470-3476.
26. Shikata, T, Hirata, H and Kotaka, T, *Micelle Formation of Detergent Molecules in Aqueous-Media - Viscoelastic Properties of Aqueous Cetyltrimethylammonium Bromide Solutions.* Langmuir, 3(6) (1987) 1081-1086.
27. Shikata, T and Kotaka, T, *Entanglement network of thread-like micelles of a cationic detergent.* J. Non-Crystal. Sol., 131-133 (1991) 831-835.
28. Cates, M E, *Reptation of living polymers: Dynamics of entangled polymers in the presence of reversible chain-scission reactions.* Macromol., 20 (1987) 2289-2296.
29. Berret, J-F, Appell, J and Porte, G, *Linear Rheology of Entangled Wormlike Micelles.* Langmuir, 9(11) (1993) 2851-2854.
30. Walker, L M, *Rheology and structure of worm-like micelles.* Current Opinion in Colloid and Interface Science, 6 (2001) 451-456.
31. Khatory, A, Lequeux, F, Kern, F and Candau, S J, *Linear and nonlinear viscoelasticity of semidilute solutions of wormlike micelles at high salt concentration.* Langmuir, 9 (1993) 1456-1464.
32. Raghavan, S R, Fritz, G and Kaler, E W, *Wormlike micelles formed by synergistic self-assembly in mixtures of anionic and cationic surfactants.* Langmuir, 18 (2002) 3797-3803.
33. Doi, M and Edwards, S F, *The Theory of Polymer Dynamics*. Oxford University Press (Oxford) (1986).
34. Granek, R and Cates, M E, *Stress relaxation in living polymers: Results from a Poisson renewal model.* J. Chem. Phys., 96 (1992) 4758-4767.
35. Cates, M E and Candau, S J, *Statics and dynamics of worm-like surfactant micelles.* J. Phys.: Condens. Matter, 2 (1990) 6869-6892.
36. Spenley, N A, Yuan, X F and Cates, M E, *Nonmonotonic constitutive laws and the formation of shear-banded flows.* J. Phys. II France, 6 (1996) 551-571.
37. Berret, J F, Roux, D C and Porte, G, *Isotropic-to-nematic transition in wormlike micelles under shear.* J. Phys. II (France)), 4 (1994) pp. 1261-1279.
38. Rothstein, J P, *Transient extensional rheology of wormlike micelle solutions.* J. Rheol., 47(5) (2003) 1227-1247.
39. Clausen, T M, Vinson, P K, Minter, J R, Davis, H T, Talmon, Y and Miller, W G, *Viscoelastic micellar solutions: Microscopy and rheology.* J. Phys. Chem., 96 (1992) 474-484.

40. Kern, F, Lequeux, F, Zana, R and Candau, S J, *Dynamics properties of salt-free viscoelastic micellar solutions.* Langmuir, 10 (1994) 1714-1723.

41. Kern, F, Lemarechel, P, Candau, S J and Cates, M E, *Rheological Properties of Semidilute and Concentrated Aqueous Solutions of Cetyltrimethylammonium Bromide in the Presence of Potassium Bromide.* Langmuir, 8 (1992) 437-440.

42. Hassan, P A, Candau, S J, Kern, F and Manohar, C, *Rheology of wormlike micelles with varying hydrophobicity of the counterion.* Langmuir, 14(21) (1998) 6025-6029.

43. Koehler, R D, Raghavan, S R and Kaler, E W, *Microstructure and dynamics of wormlike micellar solutions formed by mixing cationic and anionic surfactants.* J. Phys. Chem. B, 104(47) (2000) 11035-11044.

44. Angelescu, D, Khan, A and Caldararu, H, *Viscoelastic properties of sodium dodecyl sulfate with aluminum salt in aqueous solution.* Langmuir, 19(22) (2003) 9155-9161.

45. Chellamuthu, M and Rothstein, J P, *Distinguishing between linear and branched wormlike micelle solutions using extensional rheology measurements.* J. Rheol., 52(3) (2008) 865-884.

46. Ziserman, L, *Relationship between Rheological Properties and Nanostructure in Mixed Micellar Surfactant*, in *Dept. Biotechnology and Food Engineering*. 2005, Technion Israel Institute of Technology.

47. Drye, T J and Cates, M E, *Living netwoks: The role of cross-links in entangled surfactant solutions.* J. Chem. Phys., 96(2) (1992) 1367-1375.

48. Berret, J-F, *Transient rheology of wormlike micelles.* Langmuir, 13 (1997) 2227-2234.

49. Lee, J Y, Fuller, G G, Hudson, N E and Yuan, X-F, *Investigation of shear-banding structure in wormlike micellar solution by point-wise flow-induced birefringence measurements.* J. Rheol., 49(2) (2005) 537-550.

50. Lerouge, S and Decruppe, J P, *Correlations between rheological and optical properties of a micellar solution under shear banding flow.* Langmuir, 16 (2000) 6464-6474.

51. Decruppe, J P, Lerouge, S and Berret, J F, *Insight in shear banding under transient flow.* Phys. Rev. E, 63(022501) (2001).

52. Mendez-Sanchez, A, Perez-Gonzalez, J, de Vargas, L, Castrejon-Pita, J R, Castrejon-Pita, A A and Huelsz, G, *Particle image velocimetery of the unstable capillary flow of a micellar solutions.* J. Rheol., 47(6) (2003) 1455-1466.

53. Hu, Y T and Lips, A, *Kinetics and mechanism of shear banding in entangled micellar solutions.* J. Rheol., 49(5) (2005) pp. 1101-1027.

54. Salmon, J B, Colin, A, Manneville, S and Molino, F, *Velocity profiles in shear-banding wormlike micelles.* Phys. Rev. Letters, 90 (2003) pp. 228303-228301 - 228303-228304

55. Kadoma, I A and van Egmond, J W, *Flow-induced nematic string phase in semidilute wormlike micelle solutions.* Phys. Rev. Letters, 80(25) (1998) 5679-5682.

56. Liberatore, M W, Nettlesheim, F, Wagner, N J and Porcar, L, *Spatially resolved small angle neutron scattering in the 1-2 plane: A study of shear-induced phase - separating wormlike micelles.* Phys. Rev. E, 73 (2006) 020504.

57. Britton, M M and Callaghan, P T, *Shear banding instability in wormlike micellar solutions.* Eur. Phys. J. B, 7 (1999) 237-249.

58. Mair, R W and Calaghan, P T, *Observation of shear banding in worm-like micelles by NMR velocity imaging.* Europhys. Letters, 36(9) (1996) 719-724.

59. Cates, M E, *Nonlinear viscoelasticity of wormlike micelles (and other reversibly breakable polymers).* J. Phys. Chem., 94 (1990) 371-375.

60. Spenley, N A, Cates, M E and McLeish, T C B, *Nonlinear rheology of wormlike micelles.* Phys. Rev. Letters, 71(6) (1993) 939-942.

61. Yesilata, B, Clasen, C and McKinley, G H, *Nonlinear shear and extensional flow dynamics of wormlike surfactant solutions.* J. Non-Newtonian Fluid Mech., 133 (2006) 73-90.

62. Olmsted, P D, *Dynamics and flow induced phase separation in polymeric fluids*. Current Opinion in Colloid and Interface Science, 4 (1999) 95-100.

63. Dhont, J K G, *A constitutive relation describing the shear-banding transition.* Phys. Rev. E, 60 (1999) 4534-4544.

64. Johnson, M W and Segalman, D, *Model for viscoelastic fluid behavior which allows non-affine deformation.* J. Non-Newt. Fluid Mech., 2 (1977) 255-270.

65. Olmsted, P D, Radulescu, O and Lu, C-Y D, *Johnson-Segalman model with a diffusion term in cylindrical Couette flow.* J. Rheol, 44(2) (2000) 257-275.

66. Fielding, S M and Olmsted, P D, *Early stage kinetics in unifyied model of shear-induced demixing and mechanical shear banding instabilities.* Phys. Rev. Letters, 90(22) (2003) 224501.

67. Cook, L P and Rossi, L R, *Slippage and migration in models of dilute wormlike micellar solutions and polymeric fluids.* J. Non-Newtonian Fluid Mech., 116 (2004) 347-369.

68. Rossi, L R, McKinley, G H, Rothstein, J P and Cook, L P, *Slippage and Migration in Taylor-Couette Flow of a Model for Dilute Wormlike Micellar Solutions.* J. Non-Newtonian Fluid Mech., 136 (2006) 79-92.

69. Fischer, P and Rehage, H, *Non-linear flow properties of viscoelastic surfactant solutions.* Rheol. Acta, 36 (1997) 13-27.

70. Giesekus, H, *A simple constitutive equation for polymer fluids based on the concept of deformation-dependent tensorial mobility.* J. Non-Newtonian Fluid Mech., 11 (1982) 69-109.

71. Yuan, X F and Jupp, L, *Interplay of flow-induced phase separations and rheological behavior* Europhys. Lett., 60(5) (2002) 691-697.

72. Kumar, S and Larson, R G, *Shear banding and secondary flow in viscoelastic fluids between a cone and plate.* J. Non-Newtonian Fluid Mech., 95(2-3) (2000) 295-314.

73. Bautista, F, Soltero, J F A, Perez-Lopez, J H, Puig, J E and Manero, O, *On the shear banding flow of elongated micellar solutions.* J. Non-Newt. Fluid Mech., 94 (2000) pp. 57-66.

74. Bautista, F, de Santos, J M, Puig, J E and Manero, O, *Understanding thixotropic and antithixotropic behavior of viscoelastic micellar solutions and liquid crystalline dispersions. I. The model* J. Non-Newtonian Fluid Mech., 80(2-3) (1999) 93-113.

75. Vasquez, P, Cook, L P and McKinley, G H, *A Network Scission Model for Wormlike Micellar Solutions I: Model Formulation and Homogeneous Flow Predictions.* J. Non-Newtonian Fluid Mech., 144(2-3) (2007) 122-139.

76. Tripathi, A, McKinley, G H, Tam, K C and Jenkins, R D, *Rheology and dynamics of associative polymers in shear and extension: Theory and experiments.* Macromol., 39(5) (2006) 1981-1999.

77. Cappelaere, E, Berret, J-F, Decruppe, J P, Cressely, R and Lindner, P, *Rheology, birefringence, and small angle neutron scattering in a charged micellar system: Evidence of shear-induced phase transition.* Phys. Rev. E, 56(2) (1997) 1869-1878.

78. Berret, J-F, Porte, G and Decruppe, J P, *Inhomogeneous shear flows of wormlike micelles: A master dynamic phase diagram.* Phys. Rev. E, 55(2) (1997) 1668-1676.

79. Callaghan, P, Cates, M E, Rofe, C and Smeulders, J, *A study of the "spurt effect" in wormlike micelles using nuclear magnetic resonance microscopy.* J. Phys. II 6(1996) 375-393.

80. Santibanez, B M, Gonzalez, F R, Perez-Gonzalez, J, Acosta, L A V and Garcia, E M, *Qualitative analysis of the capillary flow stability of spurting materials by using transmitted light intensity measurements.* Revisita Mexicana De Fisica, 50 (2004) 562-568.

81. Rolon-Garrido, V, Perez-Gonzalez, J and Montalban, L V A, *Vane rheometry of an aqueous solution of worm-like micelles.* Revisita Mexicana De Fisica, 49 (2003) 40-44.

82. Grand, C, Arrault, J and Cates, M E, *Slow transients and metastability in wormlike micelle rheology.* J. Phys. II, 7 (1997) 1071-1086.

83. Schmitt, V, Marques, C M and Lequeux, F, *Shear-induced phase separation of complex fluids: The role of flow-concentration coupling.* Phys. Rev. E, 52(4) (1995) 4009-4016.

84. McKinley, G H and Sridhar, T, *Filament stretching rheometry.* Annu. Rev. Fluid Mech., 34 (2002) 375-415.

85. Prud'homme, R K and Warr, G G, *Elongational flow of solutions of rodlike micelles.* Langmuir, 10 (1994) 3419-3426.

86. Chen, C and Warr, G G, *Light scattering from wormlike micelles in an elongational flow.* Langmuir, 13 (1997) 1374-1376.

87. Fischer, P, Fuller, G G and Lin, Z, *Branched viscoelastic surfactant solutions and their responses to elongational flow.* Rheol. Acta, 36 (1997) 632-638.

88. Lu, B, Li, X, Scriven, L E, Davis, H T, Talmon, Y and Zakin, J L, *Effect of chemical structure on viscoelasticity and extensional viscosity of drag-reducing cationic surfactant solutions.* Langmuir, 14 (1998) 8-16.

89. Walker, L M, Moldenaers, P and Berret, J-F, *Macroscopic response of wormlike micelles to elongational flow.* Langmuir, 12 (1996) 6309-6314.

90. Kato, M, Takahashi, T and Shirakashi, M, *Steady planar elongational viscosity of CTAB/NaSal aqueous solutions measured in a 4-roll mill flow cell.* J. Soc. Rheol. Jpn., 30 (2002) 283-287.

91. Kato, M, Takahashi, T and Shirakashi, M. *Flow-induced structure change and flow instability of CTAB/NaSal aqueous solution in 4-roll mill flow cell*. in *Int. Congr. on Rheol.* 2004. Seoul, Korea.

92. Muller, A J, Torres, M F and Saez, A E, *Effect of the flow field on the rheological behavior of aqueous cetyltrimethylammonium p-toluenesulfonate solutions.* Langmuir, 20 (2004) 3838-3841.

93. Bhardwaj, A, Richter, D, Chellamuthu, M and Rothstein, J P, *The effect of preshear on the extensional rheology of wormlike micelle solutions.* Rheol. Acta, 46(6) (2007) 861-875.

94. Anderson, V J, Tardy, P M J, Crawshaw, J P and Maitland, G C. *Extensional flow of wormlike micellar fluids*. in *Int. Congr. Rheol.* 2004. Seoul, Korea.

95. Fuller, G G, Cathey, C A, Hubbard, B and Zebrowski, B E, *Extensional viscosity measurements for low-viscosity fluids.* J. Rheol., 31(3) (1987) 235-249.

96. Bhattacharjee, P K, Oberhauser, J, McKinley, G H, Leal, L G and Sridhar, T, *Extensional rheometry of entangled solutions.* Macromol., 35 (2002) 10131-10148.

97. Hu, Y, Wang, S Q and Jamieson, A M, *Elongational Flow Behavior of Cetyltrimethylammonium Bromide/Sodium Salicylate Surfactant Solutions.* J. Phys. Chem., 98 (1994) 8555-8559.

98. Anna, S L, McKinley, G H, Nguyen, D A, Sridhar, T, Muller, S J, Huang, J and James, D F, *An inter-laboratory comparison of measurements from filament stretching rheometers using common test fluids.* J. Rheol., 45(1) (2001) 83-114.

99. Lin, Z Q, Lu, B, Zakin, J L, Talmon, Y, Zheng, Y, Davis, H T and Scriven, L E, *Influence of surfactant concentration and counterion to surfactant ratio on rheology of wormlike micelles.* J. Colloid and Interface Sci., 239(2) (2001) 543-554.

100. Wheeler, E K, Izo, P and Fuller, G G, *Structure and rheology of wormlike micelles.* Rheol. Acta, 35(2) (1996) 139-149.

101. Meissner, J and Hostettler, J, *A new elongational rheometer for plymer melts and other highly viscoelastic liquids.* Rheol Acta, 33(1) (1994) 1-21.

102. Tirtaatmadja, V and Sridhar, T, *A filament stretching device for measurement of extensional viscosity.* J. Rheol., 37 (1993) 1133-1160.

103. Szabo, P, *Transient filament stretching rheometry I: Force balance analysis.* Rheol. Acta, 36 (1997) 277-284.

104. Szabo, P and McKinley, G H, *Filament stretching rheometer: Inertia compensation revisited.* Rheol. Acta, 42(3) (2003) 269-272.

105. Wedgewood, L E, Ostrov, D N and Bird, R B, *A finite extensible bead-spring chain model for dilute polymer-solutions.* J. Non-Newtonian Fluid Mech., 40(1) (1991) 119-139.

106. Chen, S and Rothstein, J P, *Flow of a wormlike micelle solution past a falling sphere.* J. Non-Newtonian Fluid Mech., 116 (2004) 205-234.

107. Smolka, L B and Belmonte, A, *Drop pinch-off and filament dynamics of wormlike micellar fluids.* J. Non-Newtonian Fluid Mech., 115(1) (2003) 1-25.

108. Yao, M, McKinley, G H and Debbaut, B, *Extensional deformation, stress relaxation and necking failure of viscoelastic filaments.* J. Non-Newtonian Fluid Mech., 79 (1998) 469-501.

109. Renardy, M, *Self-similar breakup of non-Newtonian fluid jets*, in *Rheology Reviews*, D.M. Binding and K. Walters, Editors. 2004, The British Society of Rheology: Aberystwyth, UK. p. 171-196.

110. Courtney, T H, *Mechanical Behavior of Materials*. McGraw Hill (Boston) (2000).

111. Joshi, Y M and Denn, M M, *Rupture of entangled polymeric liquids in elongational flows.* J. Rheol., 47 (2003) 291-298.

112. Vinogradov, G V, Malkin, A Y, Volosevitch, V V, Shatalov, V P and Yudin, V P, *Flow, high-elastic (recoverable) deformations and rupture of uncured high molecular weight linear polymers in uniaxial extension.* J. Poly. Sci. Polym. Phys. Ed., 13 (1975) 1721-1735.

113. McKinley, G H and Hassager, O, *The Considere condition and rapid stretching of linear and branched polymer melts.* J. Rheol., 43(5) (1999) 1195-1212.

114. Jayaraman, A and Belmonte, A, *Oscillations of a solid sphere falling through a wormlike micelle solution.* Phys. Rev. E, 67 (2003) 065301-065304.

115. Mollinger, A M, Cornelissen, E C and van den Brule, B H A A, *An unexpected phenomenon observed in particle settling: oscillating falling spheres.* J. Non-Newtonian Fluid Mech., 86 (1999) 389-393.

116. Handzy, N Z and Belmonte, A, *Oscillatory rise of bubbles in wormlike micellar fluids with different microstructures.* Phys. Rev. Letters, 92(12) (2004) 124501.

117. Rodd, L E, Scott, T P, Cooper-White, J J and McKinley, G H, *Capillary break-up rheometry of low-viscosity elastic fluids.* Appl. Rheol., 15(1) (2005) 12-27.

118. Anna, S L and McKinley, G H, *Elasto-capillary thinning and breakup of model elastic liquids.* J. Rheol., 45(1) (2001) 115-138.

119. McKinley, G H and Tripathi, A, *How to extract the Newtonian viscosity from capilary breakup measurements in a filament rheometer.* J. Rheol., 44(3) (2000) 653-670.

120. Stelter, M, Brenn, G, Yarin, A L, Singh, R P and Durst, F, *Validation and application of a novel elongational device for polymer solutions.* J. Rheol., 44(3) (2000) 595-616.

121. Entov, V M and Hinch, E J, *Effect of a spectrum of relaxation times on the capillary thinning of a filament of elastic liquid.* J. Non-Newtonian Fluid Mech., 72 (1997) 31-53.

122. Bazilevsky, A V, Entov, V M and Rozhkov, A N. *Liquid filament microrheometer and some of its applications*. in *Proc. Third European Rheology Conference*. 1990. Edinburgh.

123. Papageorgiou, D T, *On the breakup of viscous liquid threads.* Phys. Fluids, 7 (1995) 1529-1544.

124. Miller, E, Clasen, C and Rothstein, J P, *The effect of step-stretch parameters on capillary breakup extensional rheology (CaBER) measurements.* submitted to Rheol. Acta, (2008).

125. Miller, E, *The Dynamics and Rheology of Shear-Banding Wormlike Micelles and Other Non-Newtonian Fluids*, in *Mechanical Engineering*. 2007, University of Massachusetts: Amherst.

126. Wagner, M H, Bastian, H, Hachmann, P, Meissner, J, S., K, Munstedt, H and Langouche, F, *The strain-hardening behavior of linear and long-chain-branched polyolefin melts in extensional flows.* Rheol. Acta, 39(2) (2000) 97-109.

127. Munstedt, H and Laun, H M, *Elongational properties and molecular structure of pollyethylene melts.* Rheol. Acta, 20 (1981) 211-221.

128. Decruppe, J P and Ponton, A, *Flow birefringence, stress optical rule and rheology of four micellar solutions with the same low shear viscosity.* Eur. Phys. J. E, 10 (2003) 201-207.

129. Anna, S L and McKinley, G H, *Effect of a controlled pre-deformation history on extensional viscosity.* in press Rheol. Acta, (2008).

130. Walters, K and Tanner, R I, *The motion of a sphere through an elastic liquid*, in *Transport Processes in Bubbles, Drops and Particles*, R. Chhabra and D. De Kee, Editors. 1992, Hemisphere Publ. Corp.: New York.

131. Chhabra, R P, *Bubbles, Drops and Particles in Non-Newtonian Fluids*. Second ed. CRC Press (Boca Raton) (2007).

132. McKinley, G H, *Steady and transient motion of spherical particles in viscoelastic liquids*, in *Transport Processes in Bubbles, Drops & Particles*, R. Chhabra and D. De Kee, Editors. 2001, Taylor and Francis: New York.

133. Hassager, O, *Working group on numerical techniques, Fifth International Workshop on Numerical Methods in Non-Newtonian flows, Lake Arrowhead, USA*. J. Non-Newtonian Fluid Mech., 29 (1988) 2-5.

134. Bisgaard, C, *Velocity-fields around spheres and bubbles investigated by laser-Doppler anemometry.* J. Non-Newtonian Fluid Mech., 12 (1983) 283-302.

135. Liu, Y J, Liao, T Y and Joseph, D D, *A two-dimensional cusp at the trailing edge of an air bubble rising in a viscoelastic liquid.* J. Fluid Mech., 304 (1995) 321-342

136. Belmonte, A, *Self-oscillations of a cusped bubble rising through a micellar solution.* Rheol. Acta, 39(6) (2000) 554-559.

137. Soto, E, Goujon, C, Zenit, R and Manero, O, *A study of velocity discontinuity for single air bubbles rising in an associative polymer.* Phys. Fluids, 18 (2006) 121510.

138. Maitland, G G, *Oil and gas production.* Current Opinion in Colloid and Interface Science, 5 (2000) 301-311.

139. Chase, B, Chmilowski, W and Dang, Y, *Clear fracturing fluids for increase well productivity.* Oilfield Rev., (1997) 20-33.

140. Perrin, C L, Tardy, P M J, Sorbie, K S and Crawshaw, J C, *Experimental and modeling study of Newtonian and non-Newtonian fluid flow in pore network micromodels.* J. Colloid Interface Sci., 295 (2006) 542-550.

141. DaRocha, C M, Patruyo, L G, Ramı´rez, N E, Muller, A J and Saez, A E, Polym. Bull., 42 (1999) 109-116.

142. Koshiba, T, Hashimoto, T, Mori, N and Yamamoto, T, *Pressure loss of viscoelastic surfactant solutions under the flow in a packed bed of particles.* Nihon Reoroji Gakkaishi, 35(1) (2007) 21-26.

143. Boek, E S, Padding, J T, Anderson, V J, Briels, W J and Crawshaw, J P, *Flow of entangled wormlike micellar fluids: Mesoscopic simulations,rheology and μ-PIV experiments.* J. Non-Newtonian Fluid Mech., 146 (2007) 11-21.

144. Rothstein, J P and McKinley, G H, *The axisymmetric contraction-expansion: The role of extensional rheology on vortex growth dynamics and the enhanced pressure drop.* J. Non-Newtonian Fluid Mech., 98 (2001) 33-63.

145. Rodd, L E, Scott, T P, Boger, D V, Cooper-White, J J and McKinley, G H, *The inertio-elastic planar entry flow of low-viscosity elastic fluids in micro-fabricated geometries.* Journal of Non-Newtonian Fluid Mechanics, 129(1) (2005) 1-22.

146. Virk, P S, *Drag reduction fundamentals.* AIChE J., 21 (1975) 625-656.

147. Sureshkumar, R, Beris, A N and Handler, R A, *Direct numerical simulation of the turbulent channel flow of a polymer solution.* Phys. Fluids, 9(3) (1997) 743-755.

148. Dimitropoulosa, C D, Sureshkumar, R and Beris, A N, *Direct numerical simulation of viscoelastic turbulent channel flow exhibiting drag reduction: effect of the variation of rheological parameters.* J. Non-Newtonian Fluid Mech., 79 (1998) 433-468.

149. Ptasinski, P K, Boersma, B J, Nieuwstadt, F T M, Hulsen, M A, Brule, B H A A V D and Hunt, J C R, *Turbulent channel flow near maximum drag reduction: simulations, experiments and mechanisms.* J. Fluid Mech., 490 (2003) 251–291.

150. Dubief, Y, White, C M, Terrapon, V E, Shaqfeh, E S G, Moin, P and Lele, S K, *On the coherent drag-reducing and turbulence-enhancing behaviour of polymers in wall flows.* J. Fluid Mech., 514 (2004) 271–280.

151. Terrapon, V E, Dubief, Y, Moin, P, Shaqfeh, E S G and Lele, S K, *Simulated polymer stretch in a turbulent flow using Brownian dynamics.* J. Fluid Mech., 504 (2004.) 61-71.

152. Lin, Z Q, Zakin, J L, Zheng, Y, Davis, H T, Scriven, L E and Talmon, Y, *Comparison of the effects of dimethyl and dichloro benzoate counterions on drag reduction, rheological behaviors, and microstructures of a cationic surfactant.* J. Rheol., 45 (2001) 963-981.

153. Myska, J, Lin, Z C, Stepanek, P and Zakin, J L, *Influence of salts on dynamic properties of drag reducing surfactants.* J. Non-Newtonian Fluid Mech., 97(2-3) (2001) 251-266.

154. Lin, Z Q, Cho, L C, Lu, B, Zheng, Y, Davis, H T, Scriven, L E, Talmon, Y and Zakin, J L, *Experimental studies on drag reduction and rheology of mixed*

cationic surfactants with different alkyl chain lengths Rheol. Acta, 39(4) (2000) 354-359.

155. Stern, P and Myska, J, *Viscous and elastic properties of a cationic and a zwitterionic drag reducing surfactant* Colloids and Surfaces A - Physicochemical and Engineering Aspects, 183 (2001) 527-531.
156. Zakin, J L, Myska, J and Chara, Z, *New limiting drag reduction and velocity profile asymptotes for non-polymeric additives systems.* AIChe J., 42 (1996) 3544-3546.
157. Aguilar, G, Galsjevic, K and Matthys, E F, *Asymptotes of maximum friction and heat transfer reductions for drag-reducing surfactant solutions.* Int. J. Heat Mass Transfer, 44 (2001) 2835-2843.
158. Crooks, R and Boger, D V, *Influence of fluid elasticity on drop impacting on dry surfaces.* J. Rheol., 44(4) (2000) 973-996.
159. Cooper-White, J J, Crooks, R C and Boger, D V, *A drop impact study of worm-like viscoelastic surfactant solutions.* Colloids and Surfaces A: Physicochemical and Engineering Aspects, 210 (2002) 105-123.
160. Cooper-White, J J, Crooks, R C, Chockalingam, K and Boger, D V, *Dynamics of polymer-surfactant complexes: elongational properties and drop impact behavior.* Ind. Eng. Chem. Res., 41 (2002) 6443-6459.
161. Crooks, R, Cooper-White, J J and Boger, D V, *The role of dynamic surface tension and elasticity on the dynamics of drop impact.* Chem. Eng. Sci., 56 (2001) 5575-5592.
162. Lampe, J, DiLalla, R, Grimaldi, J and Rothstein, J P, *The impact dynamics of droplets on thin films of viscoelastic wormlike micelle solutions.* J. Non-Newtonian Fluid Mech., 125 (2005) 11-23.
163. Cheny, J M and Walters, K, *Extravagant viscoelastic effects in the Worthington jet experiment.* J. Non-Newtonian Fluid Mech., 67 (1996) 125-135.
164. Arigo, M T and McKinley, G H, *The effect of viscoelasticity on the transient motion of a sphere in a shear-thinning fluid.* J. Rheol., 41(1) (1997) 103-128.
165. Akers, B and Belmonte, A, *Impact dynamics of a solid sphere falling into a viscoelastic micellar fluids.* J. Non-Newtonian Fluid Mech., 135 (2006) 97-108.
166. Zhou, C, Yue, P, Feng, J J, Liu, C and Shen, J, *Heart-shaped bubbles rising in anisotropic liquids.* Phys. Fluids, 19 (2007) 041703.
167. Clark, C J and Dombrowski, N, *Aerodynamic instability and disintegration of liquid sheets.* Proc. R. Soc. Lond. A, 329 (1972) 467-478.
168. Dombrowski, N and Fraser, R P, *A photographic investigation into the disintegration of liquid sheets.* Phil. Trans. Roy. Soc. London A, 247 (1954) 101-130.
169. Choo, Y-J and Kang, B-S, *The velocity distribution of the liquid sheet formed by two low-speed impinging jets.* Phys. Fluids, 14(2) (2002) 622-627.
170. Taylor, G I, *The dynamics of thin sheets of fluids. III. Disintegration of fluid sheets.* Proc. R. Soc. Lond. A, 253 (1959) 313-321.
171. Xing, L-L and Glass, J E, *Parameters influencing the spray behavior of waterborne coatings.* J. Coatings Tech., 71 (1999) 3750.

172. Mun, R P, Young, B W and Boger, D V, *Atomization of dilute polymer solutions in agricultural spray nozzles.* J. Non-Newtonian Fluid Mech., 83 (1999) 163-178.

173. Stelter, M, Brenn, G and Durst, F, *The influence of viscoelastic fluid properties on spray formation from flat-fan and pressure-swirl atomizers.* Atomization and Sprays, 12 (2002) 299-327.

174. Harrison, G M, Mun, R P, Cooper, G and Boger, D V, *A note on the effect of polymer rigidity and concentration on spay atomization.* J. Non-Newtonian Fluid Mech., 85 (1999) 93-104.

175. Miller, E, McWilliams, E, Gibson, B and Rothstein, J P, *The collision of viscoelastic jets and the formation of fluid webs.* App. Phys. Let., 87 (2005) 014101.

176. Brenn, G, Liu, Z and Durst, F, *Three-dimensional tempral instability of non-Newtonian liquid sheets.* Atomization and Sprays, 11 (2001) 49-84.

177. Thompson, J and Rothstein, J P, *The atomization of viscoelastic fluids in flat-fan and hollow-cone spray nozzles.* J. Non-Newtonian Fluid Mech., 147 (2007) 11-22.

178. Stone, H A, *Dynamics of drop deformation and breakup in viscoelastic fluids.* Annu. Rev. Fluid Mech., 26 (1994) 65-102.

179. Renardy, M, *A numerical study of the asymptotic evolution and breakup of Newtonian and viscoelastic jets.* J. Non-Newtonian Fluid Mech., 59 (1995) 267-282.

180. Mun, R P, Byars, J A and Boger, D V, *The effect of polymer concentration and molecular weight on the breakup of laminar capillary jets.* J. Non-Newtonian Fluid Mech., 74 (1998) 285-297.

181. McKinley, G H, *Visco-elasto-capillary thinning and break-up of complex fluids*, in *Annual Rheology Reviews*, D.M. Binding and K. Walters, Editors. 2005, The British Society of Rheology: Aberystwyth, Wales, UK. p. 1-49.